Development of vibrational spectroscopic techniques for measuring quality-related parameters of connective tissue.

Karen Wahlstrøm Sanden

Norwegian University of Life Sciences
Department of Chemistry, Biotechnology and Food Science
Master Thesis 60 credits 2011

Acknowledgements

This work was performed at the Nofima Mat AS. The polarized FTIR measurements were done at Temple University in Philadelphia, USA.

I want to thank my great supervisor-team at Dr. Achim Kohler (IMT, Norwegian University of Life Science and Nofima Mat AS) and Dr. Mona E. Pedersen (Nofima Mat AS). Thank you for all your good advices and support, and your enthusiasm and encouragement!
I also want to thank my supervisor at the Norwegian University of Life Science, Prof. Bjørg Egelandsdal.

A special thank I would like to give to Dr. Nancy Pleshko at Temple University in Philadelphia for introducing me to a new part of the spectroscopic world, the polarized FTIR spectroscopy, and for the warm welcome in Philadelphia. Thank you very much, also to the students in Dr. Pleshko's group for the great assistance in the lab and for making my stay in USA unforgettable! I also grateful for the financial support from Nofima Mat AS for my stay at Temple University.

I want to thank Grethe Enersen for being really helpful due to the histological analysis.

Finally, I would like to thank my family and friends who have given me encouragement and support throughout this period and towards my degree.

I really appreciate all your contribution to this work. Thank you all so much.

Ås, May 2011
Karen Wahlstrøm Sanden

Abstract

The aim of this work was to study by Fourier-transform infrared (FT-IR) micro spectroscopy different parameters of connective tissue, which have previously been related to meat tenderness. These parameters were collagen fiber orientations, collagen and sulfated glycosamineoglycans (GAGs) content, and their relative ratio during storage. Two different bovine muscles were studied, *M. psoas major* (PM) and *M. Semitendinosus* (ST). These muscles are known to differ in tenderness, with the PM muscle as the most tender. The muscles were aged at 4º for 19 days and samples were taken for spectroscopic, biochemical and histological analysis every third day. Mechanical measurements (Warner Bratzler) were done to confirm the textural properties in the two muscles. Biochemical measurement by DMB and histological staining by Alcian blue were used to verify the content and distribution of sulfated GAGs in the two muscles during aging. The tissue sections were also stained with collagen I antibodies to see the distribution of collagen in the connective tissue in the two muscles.

The tissue section was measured by (FT-IR) micro spectroscopy using single spectra and polarized light microscopy imaging. The absorbance peaks obtained from single spectra were related to the connective tissue parameters, and the polarized measurement was used to investigate the direction of the collagen fibers in the connective tissue.

The sulfate stretch band at 1237 cm^{-1} in the infrared spectrum showed a decrease in sulfated GAGs in both muscles during storage, in accordance with biochemical and histological results. The ST muscle had a higher content of sulfated GAGs and had a more pronounced decrease measured biochemically, and the same result were also obtained in the spectra.

The collagen absorption band at 1659 cm^{-1}showed a possible degradation of cross-links in the PM muscle, however, using a different cross-links ratio (1660:1690) no difference were found. The absorbance at 1654 cm^{-1} could indicate a conformation change in the collagen α-helix in the PM muscle. Two bands in the water region were assigned to hydrogenated and non-hydrogenated N-H starching bands at ~3290 and ~3335 cm^{-1} respectively. These water bands could be used to estimate the hydrogenation of connective tissue proteins and shows that the water content in the samples is decreasing during storage.

The polarized measurements showed that the collagen fibers in the PM muscle had a random orientation, while fibers in the ST muscle showed an orientation parallel to the x- axis early in the period and a random orientation after 11 days post mortem storage. Staining with antibodies against collagen I supported these results, showing that the perimysium of PM had

a more diffuse staining pattern compared to the ST muscle which showed a more wavy appearance with clear thread-like like structures.

Our results from this study show that FT-IR micro spectroscopy is promising in evaluating connective tissue in bovine skeletal muscles. Good correlation between the spectroscopic measurement due to the biochemically and histological methods was obtained.

Sammendrag

Målet med dette arbeidet var å studere ulike parametre av bindevev med Fourier-transform infrarød (FT-IR) spektroskopi. Disse parametrene er kollagen fiber orientering, kollagen og sulfaterte glykosamineoglykaner (GAGs) mengde, og deres relative ratio under lagring. To ulike bovine muskler ble studert, indrefilet (M. *psoas major*, PM) og lårtunge (M. *semitendinosus*, ST). Disse musklene varierer i mørhet, der indrefilet er mørest. Musklene ble lagret ved 4 º i 19 dager, der prøver ble tatt ut hver tredje dag til spektroskopiske, biokjemiske og histologiske analyser. Mekanisk målinger (Warner Bratzer) ble gjort for å bekrefte tekstur egenskaper i de to musklene. Biokjemisk måling med DMB og histologisk farging med Alcian blue ble brukt til å måle innhold og detektere fordelingen av sulfaterte GAGs i de to musklene under lagring. Prøvene ble også farget med kollagen I antistoffer for å se distribusjonen av kollagen I i bindevevet i de to musklene.

Prøvene ble målt med FT-IR mikro spektroskopi og ved hjelp av både enkelt spektra og polarisert lysmikroskopi avbilding. Absorbans topper ble analysert i forhold de ulike bindevevsparameterne. De polarisert målingen ble brukt til å undersøke retningen av kollagen fibrene i bindevevet.

Absorbans topp ved 1237 cm^{-1} viste en nedgang i sulfaterte GAGs i begge muskler under lagring, dette i samsvar med biokjemiske og histologiske resultater. Lårtunge hadde et høyere innhold av sulfaterte GAGs enn indrefilet. Lårtunge hadde også en mer markant nedgang som ble sett både i de biokjemiske resultatene og i spektrene.

Absorpsjon av collagen ved 1659 cm^{-1} viste en mulig degradering av kryssbindinger i indrefilet, men ved bruk av en annen kryssbinding ratio (1660:1690) ble ingen forskjell funnet. Absorbansen ved 1654 cm^{-1} kan indikere en konformasjon endring i kollagen α-helix i indrefilet. To band i vannet regionen viste hydrogenert og ikke-hydrogenert N- H strekk, på henholdsvis ~ 3290 og ~ 3335 cm^{-1}. Disse vann toppene kan brukes til å beregne hydrogenering av bindevevs proteiner og det viser at musklene mister vann gjennom lagring.

De polariserte målingene viste at kollagen fibrene i indrefilet hadde en tilfeldig orientering, mens fibre i lårtunge viste en orientering parallelt med x-aksen tidlig i perioden, og en tilfeldig orientering etter 11 dagers lagring.. Farging med antistoffer mot kollagen I støttet disse resultatene, viser en mer tydelig kollagen orientering med ”trådlike” strukturer.

Våre resultater fra denne studien viser at FT-IR mikro spektroskopi er lovende i evaluering av bindevevs komponenter i bovine skjelett muskler. Det var god korrelasjon mellom de spektroskopiske og biokjemiske målingene.

Table of Contents

1 Introduction

Meat as meat cuts are one of the most important food resources. Skeletal muscle is a composite structure comprised of contractile myofibers attached by connective tissue. The properties of both the myofibers and the connective tissue are important for texture of meat. There is great variability in tenderness of meat both between animals and between different muscles from the same animal (Nishiumi, *et al.* 1995, Sink, J. *et al.* 1983).
Myofibers and their relation to tenderness have been extensively studied (Tornberg, E.,1996, and Harper, G.S., 1999). Connective tissue contains both collagen and proteoglycans (PG) as predominant components. Collagen content, collagen phenotypes as well as amount of crosslinks have been studied (Bailey and Light, 1989). The content of PGs and the structural organization of them are also contributing to the tenderness of beef. The PGs consist of a protein core and linear unbranched polysaccharide chains named glycosamineoglycans (GAGs). The GAGs can be sulfated or non-sulfated (Bailey and Light, 1989, Light*, et al*., 1985, Nishimura, *et al.*1996, Eggen *et al.* 1998).
Different methods that involve chemical and biochemical techniques are used to measure quality parameters of connective tissue. The content of sulfated GAGs is measured biochemically. The amount of collagen cross-links can be measured with high-performance liquid chromatografi (HPLC) (Pashalis *et al*.2001) or their solubility by use of different extraction methods (Eggen *et al* 2001), proven useful as an indicator of connective tissue softening (Uldbjerg, *et al.* 1983). The tenderness of beef is mostly measured mechanically. These are all accurate methods, but require much sample preparation and are therefore time consuming.

Fourier-transform infrared (FT-IR) micro spectroscopic imaging techniques are powerful and fast methods for analyzing biochemical composition in a large number of samples. The wavelengths of many IR absorption band are characteristic of specific types of chemical bands, and molecular structure information about non-organic and organic components (Socrates, G., 2001) can be identified. It has been extensively used in investigation and identification of pathological tissues (Bi, X. 2007, Camacho, N.P. 2001) with focus on changes in connective tissue of cartilage and bone. The PG content and distribution in these tissues have been determined using Fourier-transform infrared imaging spectroscopy (FT-IRIS). FTIR imaging of PG was demonstrated to correlate with usual histological staining of PG in cartilage. Polarized light microscopy has been used to evaluate the collagen orientation

in connective tissue of cartilage. The ratio AmideI/Amide II grouped the categories of orientation in three groups after careful examination between polarized light microscopy and FT-IRIS (Bi, et al 2007). In this study, also composition and degradation of connective tissue components as collagen and proteoglycans of bone and its relation to disease was evaluated by FTIR. Type and amount of collagen crosslinking of bone tissue/cartilage has also proven possible by FTIR analysis (Pashalis *et al*.2001).

In this experiment we want to study the correlation of FTIR analysis with different connective tissue parameters, parameters that have been studied in relation to tenderness of bovine skeletal muscle. The parameter is selected due to parameters that have shown change during post mortem storage. The connective tissue from two different bovine muscles, differing in texture properties, *M. psoas major* and *M. semitendinosus*, has been investigated by FT-IR micro spectroscopy and polarized light microscopy. The content of sulfated GAGs has been measured biochemically and used as a reference analysis. Histological staining has been done to support these result. This kind of study has never been done on bovine tissue before. The collagens and sulphated GAGs during post mortem storage was also invistegated by FT-IR.

2 Background

2.1 Muscles structure

The muscle fibers are multinucleated giant cells, aligned into long parallel bundles. Each muscle cell (myofiber) contains long tube like organelles called myofibrils which run the length of the muscle cell. These are the contractive element of muscle, organized into thick and thin filaments. The thick filaments consist of myosin, and thin filament consists of actin. These contractile elements make up a sarcomere. Muscles fibers consist of a numbers of sarcomeres. The thin filaments are anchored at one end in a structure, the z-disk, oriented perpendicular to the thin filaments. The Z-line is composed of Z-filaments that serve as bridges between the thin filaments of adjacent sarcomeres (Jugde, *et al.* 1989).

Connective tissue surrounds each individual muscle fiber, and also the bundles of muscle fibers and the whole muscle (figure 1). It is a dynamic framework with a primary role to give mechanical strength and support for tissue and to influence tissue structure and function by regulating cell behavior (Bailey, A and Light, N. 1989).

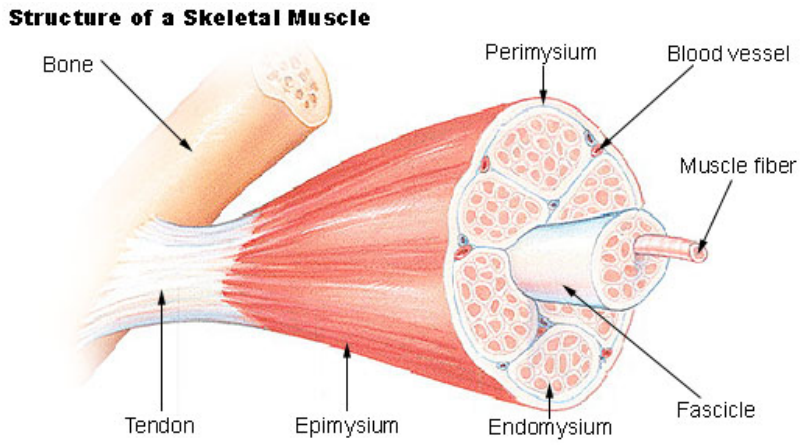

Figure 1: Skeletal muscle organization, showing the epi, peri and endomysium. (http://upload.wikimedia.org/wikipedia/commons/8/89/Illu_muscle_structure.jpg)

The location of the muscle in the animal can affect the tenderness and adaption to mechanical properties (Jugde, M et al., 1989).
Two muscles with differences in location show different textural properties. The *M. psoas major* (PM) is known to be a more tender muscle than M. *semitendinosus* (ST). Figure 2 shows the location of PM and ST on the carcass. .

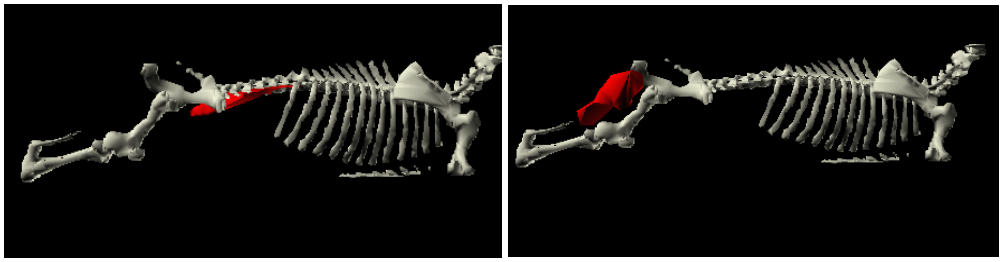

Figure 2: The location on PM (left) and ST (right) on the carcass (http://bovine.unl.edu/bovine3D/eng/3did.html).

2.2 Connective tissue

Unlike other tissue types that are formed mainly by cells, the major constituent of connective tissue is its extracellular matrix (ECM), composed of collagen, elastic fibers, glycoproteins and proteoglycans.

2.2.1 Collagen

The collagens are a large family of molecules. Each collagen molecule is composed of three polypeptide chains which form a unique triple helical structure. The chains are composed of repeating unit of –Gly-Xaa-Yaa, where Xaa and Yaa can be any amino acid but are frequently the imino acids proline and hydroxyproline (Kadler, *et al.* 1996.). The collagen molecule contains about 33 % of the amino acid glycine, 12 % proline and 11 % hydroxy-proline.
The different chains are designated α1, α2, α3. The chains of a collagen molecule can be similar or different, depending on the type of collagen.
The chain is stabilized by H-bonds. For the three chains to wind into a triple helix they must have the smallest amino acid, glycine at every third residue along the chain (Kadler, *et al.*1996).

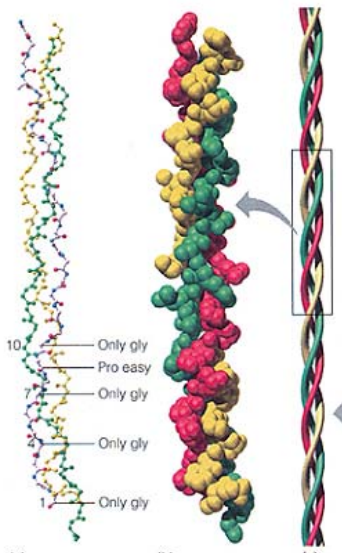

Figure 3: Collagen molecule.
https://chempolymerproject.wikispaces.com/Collagen-D-apml

2.2.2 Collagen types and organization

Connective tissue envelopes muscles, muscle bundles and muscle fibers. The endomysium is the fine connective tissue layer separating individual muscle fibres. The vast majority of its thickness is made up of a near- random feltwork of fine, wavy collagen fibres. This collagen feltwork can easily reorientate with changing the muscle length (Purslow and Trotter, 1994). The connective tissue layer that separates each muscle into muscle fiber bundles, or fascicles is the perimysium. There are large (primary) fascicles and smaller (secondary) fascicles. Primary and secondary perimysiums are arranged in a crossed-ply arrangement of two sets of wavy collagen fibers (Rowe, R. 1981). Reorientation of this collagen network allows the perimysium to easily follow elongation or shortening of the muscle fascicles. The epimysium is the connective tissue sheath delineating and separating individual muscle. In many muscles collagen fibers in the epimysium are arranged into a crossed-ply arrangement of two sets of wavy collagen fibers or in muscles where the epimysium clearly participates in transferring load to adjacent structures (e.g bovine semitendinosus), the collagen fibers are more close-packed and longitudinally arranged, like a tendon (Purslow, P. 2005).

Collagen can be divided into three major groups; fibrous collagen (types I, II and III), nonfibrous collagen (type IV / basement collagen) and microfibrillar collagen (types VI, VII, V IX, X), VIII and XI)(Youling L. Xiong). The microfibrillar collagen molecules form a loosely packed filamentous structure with anti-parallel alignment of individual molecules. Type IV collagen molecules are the only members of the non-fibrous category found in the muscle. They form a "chicken wire" structure, which can be found in basement membranes (Weston, *et al*. 2002).

The fibrous collagen self- assembles to form a characteristic band pattern. The formation of collagen fibril is shown in figure 4.
The fibrous collagen is created by monomers of tropocollagen molecules. Tropocollagen is a long thin molecule with a molecular weight of 300000 Da and a length of 280 nm (Weston*, et al*. 2002).
Each tropocollagen molecule overlaps its lateral counterpart by slightly less than one-fourth of its length and is aligned in a quarter – stagger fashion (similar to building bricks). Each unit extends about three- quarters the length of its neighbor and is bonded together at frequent intervals to prevent sliding under tension. These bonds are referred to as crosslink (Bailey, A.J. 1972).

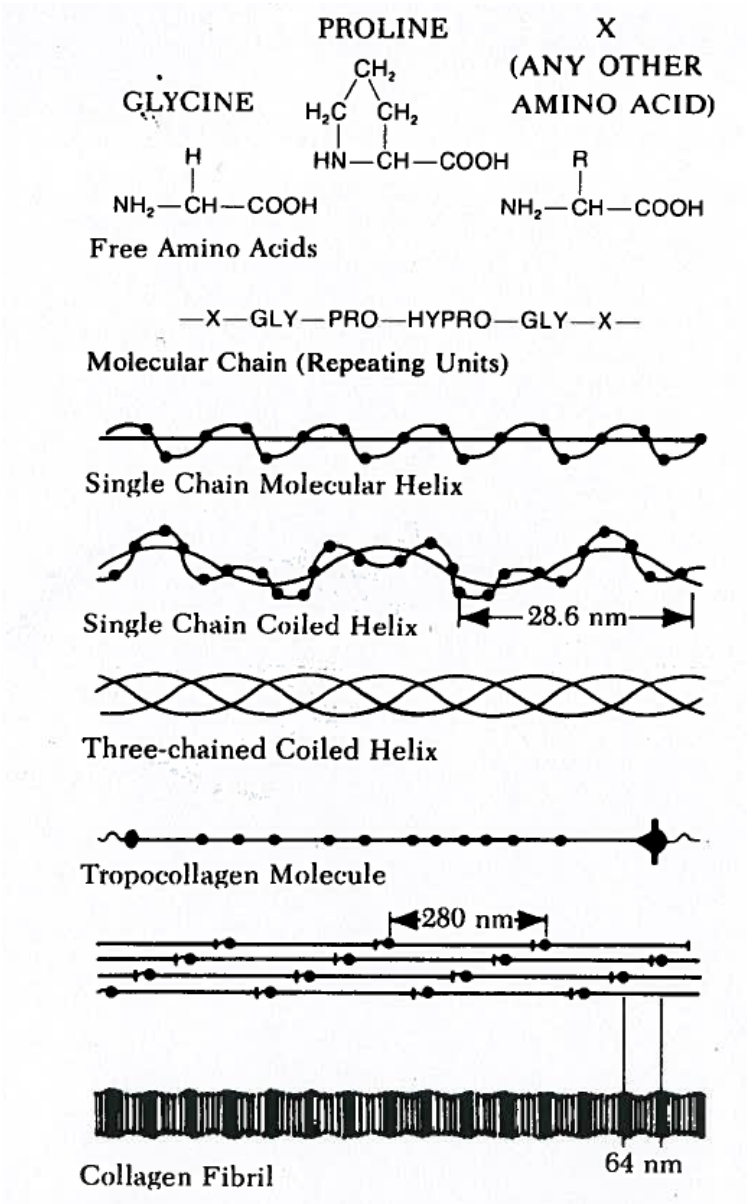

Figure 4: Diagrammatic illustration of the molecular structure of collagen, tropocollagen and the amino acid sequence. It shows the collagen fibril formation (Jugde, M et al., 1989).

After the collagen molecules are synthesized, they are secreted from the cell and into the extracellular space and align into a quarter-stagger array. Larger fibrils are formed by crosslinking between the fibrils (Reiser *et al*. 1992).

2.2.3 Biochemical property

Fibril collagens have unique biomechanical properties. The collagen fibers have a high tensile strength due to intra- and intermolecular cross-linkages. Intramolecular cross-linkages are those which are formed between the α-chains within the same molecules. Intermolecular cross-linkages are formed between α-chains in different molecules (Bailey and Light, 1989 p. 79). Intermolecular cross links are important in the stabilization of the collagen fibers (Weston, *et al*. 2002).

The collagen molecules are cross-linked internally and to other collagen molecules by different mechanism. Intra- or inter molecular disulfide bonds are confined to a few collagen types such as type III and type IV. In collagen type III molecules three cysteine side chains are present, one in each α-chain. It is possible for two of these residues to react intra-molecularly to form a disulphide bridge. The third free cysteine side chain can make intermolecular disulphide bonds with other cysteins in adjacent type III molecules (Bailey and Light, 1989 p. 79).

Collagen crosslinks with divalent bonds link two collagen chains in the same or different molecules. This is initiated by the enzyme lysyl oxidase which converts the amine group of lysine or hydroxylysine residues in the non-helical N- and C- terminals of each α-chains region into aldehydes. The aldeydes derived from lysine and hydroylysine are called allysine and hydroxallysine. Allysine and hydroxallysine react with the amino group of hydroxylysine in an adjacent collagen molecule, where allysine forms an aldimine bond and hydroxyallysine form a ketoamide bond. The aldimine bond contains a double bonded system formed between the amino nitrogen and the aldehyde carbon (fig. 5). The aldimine bond is stable under physiological condition but is disrupted by heat and low pH. The aldimine bond can therefore be chemically reduced with agents such as sodium borohydride (fig. 5). The ketoamide bond is stable at both low pH and high temperatures (Bailey and Light, 1989 p 79-89).

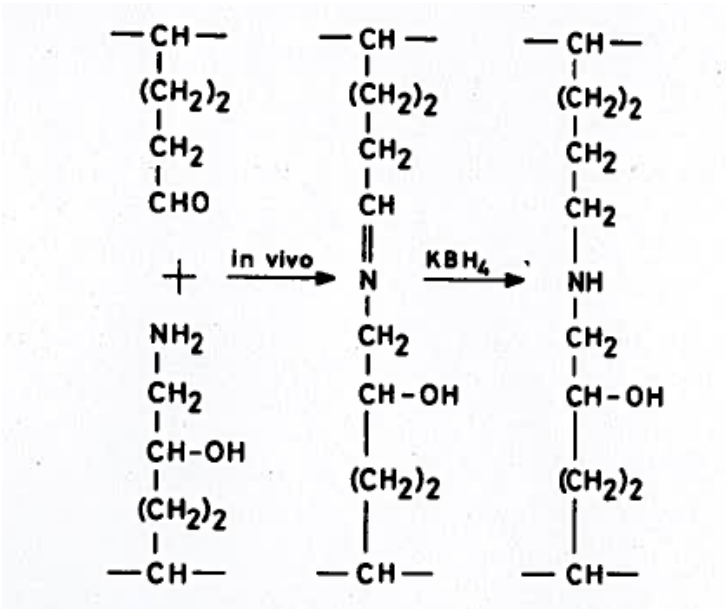

Figure 5: The formation of the aldimine bond: A double bond between the amino nitrogen and the aldehyde carbon is formed during cross-linking. The bond is reducible at low pH and when heated (Bailey and Light, 1989 p 84).

During age the collagen matrices become stronger and more rigid. One might expect that this is not because of formation of more reducible cross-links; however, it has actually been shown that the number of reducible cross-links decreases during aging. It is suggested that these cross-links were not disappearing but where further reacting with other components to be more complex and non-reducible. The non-reduible crosslinks forms trivalente and tetravalente cross-links. The divalente aldimine cross-links can for example react with histedine in a third molecule to form a trivalent cross-link which is non-reducible. The content of non-reducible and heat stable cross-links increases with age of the animals as shown in figure 6 (Bailey and Light,1989 p 89-90).

.

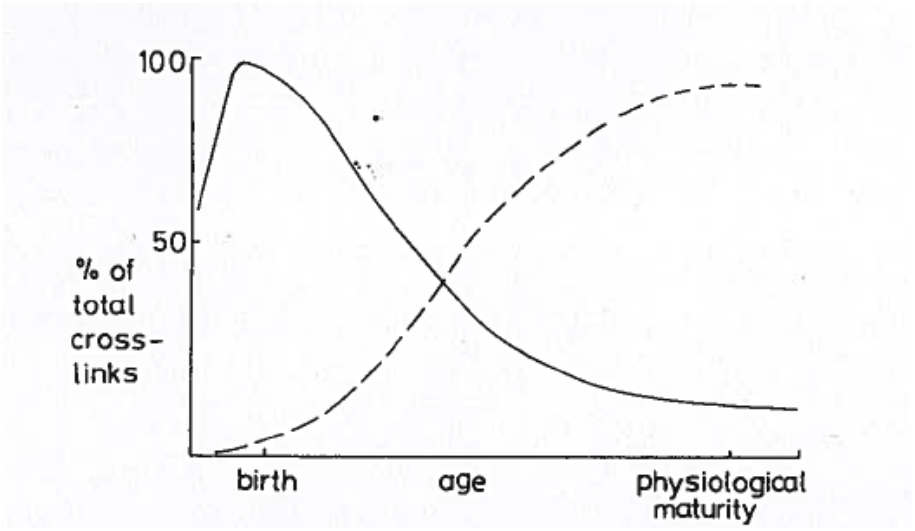

Figure 6: Changes in cross-linking in collagen during aging are shown. —— = reducible crosslinks, ———— = non-reducible mature crosslinks (Bailey, A and Light, N. 1989 p 90).

The content of collagen cross-links can be measured quantitative with high-performance liquid chromatografi (HPLC) after the collagen is prepared from a tissue homogenate, reduced and hydrolyzed with acid/alkali (Pashalis *et al*.2001). An extraction methods of collagen due to HOAc and HOAc added pepsin , has also proven useful as an indicator of connective tissue softening reflecting collagen properties (Uldbjerg 1983), and indirect some information about collagen crosslinking. This method has been used to evaluate collagen properties in two muscles differing in texture properties(Eggen *et al* 2001), .
Different staining methods as Picorius red (Junquiera *et al*., 1979) and staining by antibodies can be used to determine the distribution of collagen. The Picorius red method has also proven quantitative of collagen amount in tissue section.

2.3 Proteoglycans

Proteoglycans are complex and multifunctional molecules consisting of a protein core with variable number of covalently attached carbohydrate side chains. The polysaccharide chains are named glycosaminoglycans (Esko *et al*. 2009). Examples of some ECM proteoglycans are showed in figure 7. The structural diversity due to disaccaride composition gives the

proteoglycans unique features and functions. The number of attached GAGs chain varies from only one (e.g., decorin) to more than 100 chains (e.g., aggrecan) (Esko *et al*. 2009).

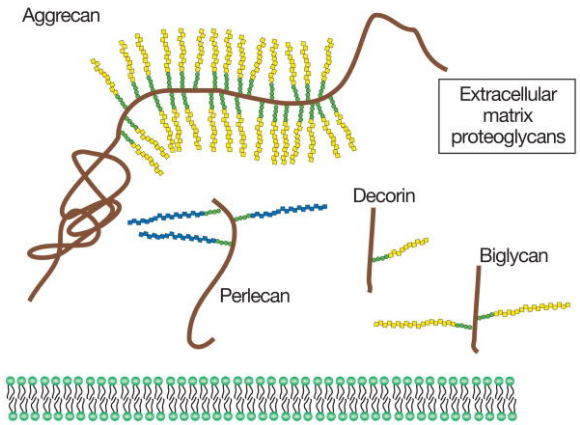

Figure 7: Some ECM proteoglycans. The proteoglycans consist of a protein core (brown) and one or more covalently attached glycosaminoglycan chains (blue and yellow)(Esko et al. 2009)

Proteoglycans have a variety of biological functions, they act as tissue organizers, influence cell growth and maturation of specialized tissue, play a role as biological filters and modulate growth-factor activities, regulate collagen fibrillogenesis and skin tensile strength, affect tumor cell growth and invasion, and influence corneal transparency and neurite outgrowth (for review Iozzo, 1998).

2.3.1 Glycoaminoglycans (GAGs)

Glycoaminoglycans (GAGs) are linear unbranced polysaccharide chains consisting of repeating disaccharide units of amino sugar (N-acetylglucosamin or N-acetylgalactosamine) and an uronic acid (glucuronic acid or iduronc acid) or galactose. The GAGs can be dived into sulfated and non – sulfated. The carboxylate and sulfate groups give the molecules strong ionic properties that make them able to attract water (Esko *et al*. 2009).

The sulfated GAGs in mammals consist of heparan sulfat (HS), chondrotin sulfat (CS)/dermatan sulfat (DS), keratan sulfat (KS) and the non-sulfated hyaluronic acid (HA).

The CS disaccharide unit contains D-glucoronic acid and N-acetylgalactosamine which usually carrying one sulfate group per disaccharide, predominantly in the 4 th (C4S) or 6 th (C6S) position of the hexoamin residue. DS is a structural isomer of CS, some of the glucuronate residues are epimerized to iduronic acid. KS is the only GAG that not contains hexuronic acid, instead there are galactose residues. The GAG hyaluronan (HA) is non-sulfated and is the only GAG that is not a part of a proteoglycan molecule. HA is a strong water binding molecule that interacts with large proteoglycans forming huge aggregates in the tissue (Esko *et al*. 2009).

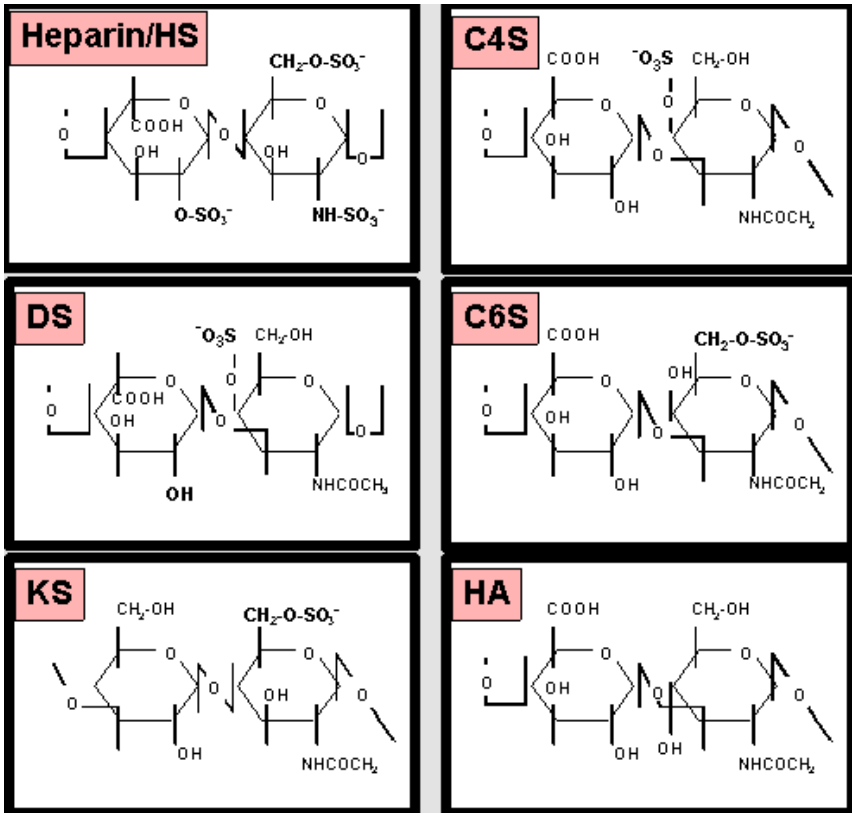

Figure 8: Schematic structures of GAGs, which is linear unbranched polysaccharide chains consting of repeating disaccharide. HS, CS, DS and KS is sulfated and the HA in non-sulfated.

GAGs have a high structural diversity due to modification steps, involving sulfation at different positions and epimerization of the glucuronic acids (GlcA) to iduronic acids (IdoA). IdoA has a major effect on the binding properties, because it can take up more than one ring confirmation and increase the conformational flexibility of the polymer (Casu *et al*., 1988).

Under physiological condition many proteins that bind to DS or HS do not bind to CS with lack the IdoA.

2.3.2 Proteoglycan distribution and interaction

The proteoglycans are distributed on cell surface, in basement membranes, extracellular matrix (ECM) and in intracellular granules.

Cell surface proteoglycans

Heparan sulfate proteoglycans (HSPGs) are dominating proteoglycans on the cell surface. The GAGs are anchored to the cell surface through a transmembran core protein called syndecans or via a glycosylphosphattidylinositol linkage as glypicans (Carey, D. 1997). They been suggested to transduce information between ECM and the inside of the cell, as matrix receptors for anchoring the cell to ECM, as co-receptors regulating cell behavior by binding and presenting growth factors and adhesion molecules (Jalkanene *et al.,* 1991).

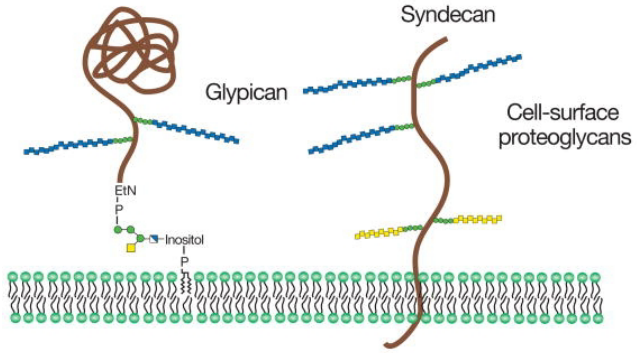

*Figure 9: Cell-surface proteoglycans (*Esko *et al*. 2009*)*

Basement membranes proteoglycans

Basement membranes are biochemically complex and heterogeneous structures containing laminin, collagen type IV, nidogen and proteoglycans. The most common proteoglycans are perlecan, agrin and bamacan. The first two carry heparan sulfate side chains and the latter carries chondroitin sulfate (Iozzo, R., 1998). The presence of heparan sulfate proteoglycans has been shown in skeletal muscle (Campos *et al*., 1993), and perlecan is found in the basement membrane area of the endomysium (Eggen *et al*., 1997).

Perlecan is essential for matrix integrity and functions in cell attachment in basement membranes, binding to other basement membrane molecules such as laminin and collagen IV. It can also interact with growth factors and can act like a crosslinker of ECM components and cell surface molecules (Iozzo, R., 1994)

Extracellular matrix proteoglycans

In contrast to cell surface and basement membrane, where HSPGs are the dominating proteoglycans, CS/DS and KS-proteoglycans are the major PGs of ECM. The ECM proteoglycans can be divided into two main groups; large and small proteoglycans.

The large group of proteoglycans is often called hyalectans, which is proteoglycans interacting with hyaluronan and lectins (Iozzo, R., 1998). They consist of a family that includes aggrecan, versican, neurocan and brevican. They all have a tridomain structure, an N-terminal domain that binds hyaluronic acid (HA), a central domain that carries the glycosaminoglycans side chain and a C-terminal region with a lecitin domain. Aggrecan is showed as an example in figure 12. Aggrecan is the main proteoglycans of cartilaginous tissue (Iozzo, R., 1998).

Aggrecan can form enormous aggregates and can contain up to 100 CS- chains in the domain II. Each aggrecan molecule is highly sulfated and creates a negative charge within the network of collagen fibers, which increase the water binding capacity.
The major functional role for the hyalectans is to bind complex carbohydrates such as hyaluronan. The lecitin domain of versican and aggrecan bind galactose and fucose (Halberg *et al*., 1988).

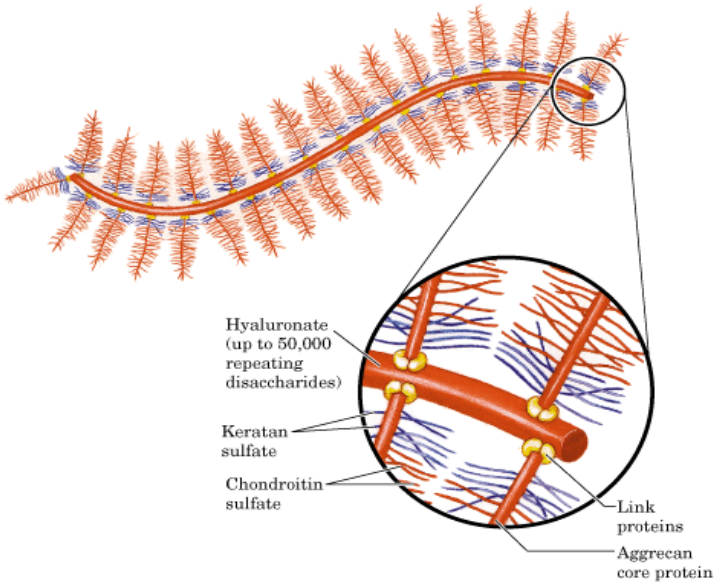

Figure 10: Shows the bottle brush like structure of proteoglycans aggregate. The aggrecan core protein interacts with hyaluonate.

The chemical property of aggrecan makes it able to bind water, and the main role in cartilage is to maintain the hydration of the tissue by attracting and binding water to give the cartilages its ability to resist compression. This property of attracting water comes from the high density of negative charges that are associated with the GAG chain (Maroudas et al., 1969). Aggrecan appears to be trapped within the collagen network of cartilage as the result of the formation of aggrecan complexes with hyaluronan and link protein (Bolis et al., 1989).
Aggrecan is known to interact with HA as shown in figure X and Y (Hannesson *et al*, 2003)

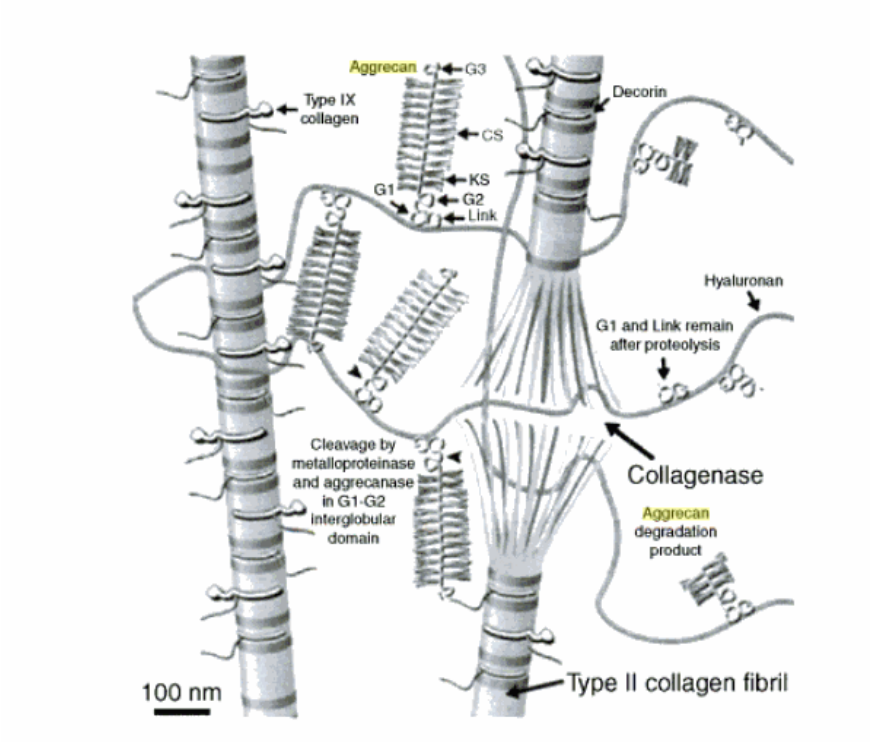

Figure 11: Structure of collagen and the proteoglycan aggrecan (Recklies, A.D, Poole, A.R., Banerjee, S. et al. 2000)

The non- aggregating small leucine proteoglycans contain only a few GAG chains, they are built up of negative charged GAGs or tyrosine residue modified with sulfate in the N-terminal end (domain I and II). They have characteristic leucine-rich repeats (LRR) domain that are located in the middle (domain III), flanked by small cysteine-clusters (domain IV). Decorin, fibromodulin and biglycan are some members of the small proteoglycans family. They have different GAGs- composition, decorin and biglycan are CD/DS proteoglycans and fibromodulin is a KS proteoglycans.

The major function of the LRR domain is to interact with other proteins. Decorin binds to almost all types of collagen either through its core protein or GAG chain. The binding site of decorin for collagen is located in the cysteine-free central domain of the core protein (Svensson *et al.,* 1995).

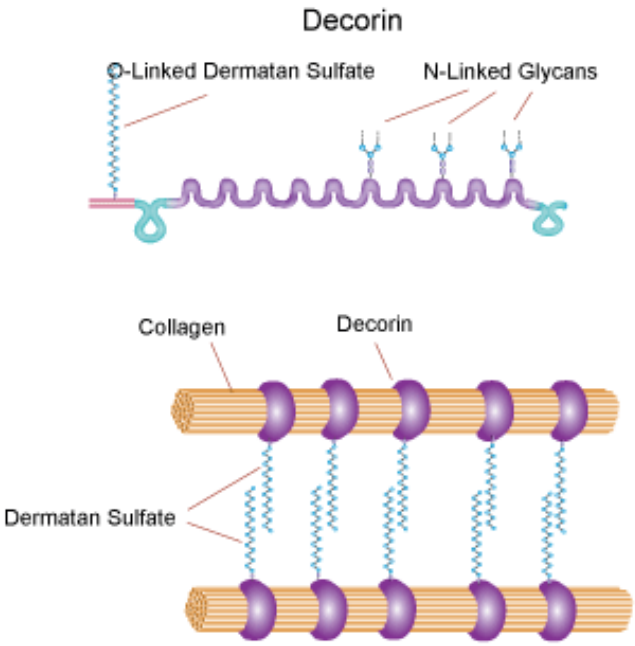

Figure 12: The small leucine proteoglycans decorin and collagen (http://www.sigmaaldrich.com/life-science/metabolomics/enzyme-explorer/learning-center/structural-proteins/decorin.html).

Decorin is considered a key regulator of matrix assembly because it regulates collagen fibrillogenesis. Evidence that decorin plays a role in collagen fibrillogenenis in animals was provided by the observation that decorin-deficient mice have fragile skin that is not able to withstand sudden tensile strains. Electron microscope examination of the skin in decorin knockout mice shows that, in the absence of decorin, collagen fibrils are coarse, irregular and haphazardly arranged. Theirs changes was accompanied by a decrease in collagen-bound PG in the skin and tendon (Danielson *et al*. 1997).

It has been suggested that fibromodulin functions as a modulator of collagen fibrillogenesis. Similar to decorin, fibromodulin binds to type I and II collagen but at a different site on each collagen molecule. Unlike decorin it promotes formation of mature large collagen *fibrils in vitro* and *in vivo* (Jepsen K.J. *et al.* 2002). It has been demonstrated that bovine skeletal muscle contains both decorin and fibromodulin (Eggen *et al.,* 1994).

2.3.3 Type and amount of collagen and proteoglycans in bovine skeletal muscle

In skeletal muscle, type and amount of collagen differ between muscles within the same animal. The collagen type I is distributed at all levels in the muscle connective tissue, while the type III collagen is present in the perimysium and the endomysium. Type I dominates in perimysium, in endomysium the level of type I and III is roughly equal. The type IV and V collagen is present in muscle endomysium (Bailey and Light, 1989 p 139).
The total content of collagen in *Psoas major* (PM) and *Semitendinosus* (ST) and the distribution of collagen in epimysium, perimysium and endomysium are shown in table 1 as measured by Bailey and Light, 1989. The collagen content in ST is higher, it is considered to be a tougher muscle than PM. In PM most of the collagen is present in the perimysium, while in the ST muscle the collagen is more equal distributed in the different connective tissue

Table 1: The content and distrubution of collagen in Psoas major (PM) and Semitendinosus (ST) (Bailey and Light, 1989 p.175).

Muscle	Total collagen (% dry wt)	Collagen in epimysium (%)	Collagen in perimysium (%)	Collagen in endomysium (%)
PM	2.24	15	79	24
ST	4.75	29	54	41

The collagen content in the perimysium varies much more between muscles than endomysial content. In a study of six bovine muscles, Light et al. (1985) show a range of 1.4-7.0 % in perimysial mass as a percentage of muscle dry weight but only a range of 0.1 – 0.5% in endomysial mass between six beef muscles. Brooks and Savell (2004) reported that perimysial thickness in bovine *Semitendinosus* muscle is on average 2.4 times thicker than in *Psoas major* from the same animal. Studies have shown that thicker perimysium is associated with reduced tenderness (Swatland *et al*., 1995).

Collagen I forms large strong fibers whilst collagen III forms thinner fibers often associated with elastic tissue. Collagen type IV does not form fibers but an amorphous “chicken-wire” network that is mostly found in the basement membranes (Bailey and Light 1989 p. 179). In

cattle an increase in the proportion of type III collagen versus to type I give tougher muscles in some animals (Bailey *et al.,* 1979).
The content of collagen type III content in PS and ST has been calculated as 0.6 % and 1.5 % of dry weight by Locker, *et al,.* (1987).

Morphological studies by transmission electron microscopy have been performed on connective tissue sections taken from adult muscles with different textural scores from the same individual. It was demonstrated that ST and PM showed a different organization of connective tissue (Eggen *et al*. 2001). The size of the collagen fibril was significant larger in ST and the organization pattern of fibrils and bundles was different in the two muscles. The tougher muscle contained regularly arranged and tightly bundled fibrils with a larger diameter. Earlier it has been demonstrated that there is a correlation between collagen diameter and texture on tissue homogenates (Light *et al*. 1985). In the tender muscle it was observed a looser network of thin collagen fibrils with larger space between the fibrils. In the tougher muscle the collagen fibrils were arranged in an organized network with fibers running in different direction. The fibril bundles were also detected in the tender muscle but it was more randomly arranged.
Changes in organization and thickness of collagen fibers were furthermore found during development of bovine skeletal muscle by scanning electron microscopy, and were closely related for mechanical strength (Nishimura, 1996).

The amount of heat stable collagen cross-links is a factor that influences the toughness of meat. ST has a much higher content of cross-links presented in the perimysium than the more tender muscle PT (Bailey and Light, 1989 p 181).

The structure and composition of the GAG chain strongly influence the mechanical properties of connective tissue (Fransson and Cøster, 1979). There are differences of amount of GAGs and the type of GAGs in different muscles. Studies done by Pedersen et al. (1999) show that the amount of DS (EMC proteoglycans) is higher in the tougher muscle ST than in PM.
In previous studies done by Pedersen et al. (1999) there were no significant difference in the total amount of GAGs measured by hexuronic acid in ST and PM, but there were a significant difference in the ratio of GAGs/OH-proline between the two muscles. The difference in content of sulphated GAGs (reflecting measurement without HA) is unknown. The tougher muscle exhibited a lower GAG/OH proline ratio. OH-proline represent mainly the collagen

fibers, and the GAG represent the matrix around the fibers, the GAG/OH proline ratio could be an indicator for the density of the connective tissue of the muscle (Pedersen et al. 1999).

Both fibromodulin and decorin is present in bovine skeletal muscle. The tougher muscle, ST contained significantly more decorin than the tender muscle PM, but less decorin per collagen. The differences in fibromodulin level per collagen showed a similar pattern, but in contrast to decorin this difference was not significant between ST and PM (Pedersen et al., 2001). Aggrecan like proteoglycans is also demonstrated to be present in ST muscle (Eggen et al., 1994

2.3 Connective tissue degradation

Muscles are active components of the body, responsible for locomotion under strict control of the nervous system and well supplied with oxygen and nutrients. After slaughter of an animal, muscle become isolated structures with no supply of oxygen and nutrients. Many of the biochemical reactions present in the living state retain. Due to residual intracellular glucose and glycogen, glycolysis continues for some time. In absence of oxygen the final product of glycolysis is lactic acid, which accumulates and induces a decrease in the pH of the muscle. The contractile apparatus, deprived of its store of adenosine triphospate (ATP), goes into a state of excessive and uncontrolled contraction called rigor mortis (the stiffness of dead). The muscle does not remain in this "stiffened" state but becomes soft due to a series of enzymatic degradation (Bailey and Light, 1989 p.13).

Water holding capacity: The term water holding capacity is defined as the ability of meat to retain its water during application of external forces (Offer and Knight, 1988).
A tissue with poor water holding capacity will loose moisture and weight. The meat will shrink during storage. The water molecules are polar and can associate with electrically charged reactive groups of muscle proteins. When the pH reaches the isoelectric point (~ pH 5) of actin and myosin, there will be an equal number of positively and negatively charged

groups. At this point the groups tend to be attracted to each other, and there will be few groups that are available for water binding.
The water- holding capacity also depends on the collagen content in the muscle.
The swelling of collagen on either side of its isoelectric point has been well investigated. It has been shown that when the swelling increases, the tensile strength of the fiber decreases, and the collagen is more label to heat (Bailey and Light 1989 p177).

Connective tissue, where collagen is the dominating component plays a role in meat quality. Collagen form strong fibrous structures linking muscle elements together, therefore it is hypothesized that the total amount of this component determines the meat texture.
It has been suggested that collagen with large fiber diameters and highly packed bundles contribute to tough meat. The bundles and the thick collagen fibers are more difficult to damage by proteases during storage.

Eggen et al. have described decorin and a large dermatan sulfate proteoglycans in bovine skeletal muscle which were degraded during post mortem storage (Eggen et al., 1994, Eggen et al. 1998., Eggen and Buer, 1991).
The large proteoglycan with aggrecan characteristic has been shown to be degraded the first 24 h after slaughter (Eggen *et al,.* 1994)) post mortem. It was shown by measuring the amount of GAGs in different fraction after gel column chromatography. It was also demonstrated that GAG containing material of high molecular size as HA was degraded.

The tenderness of meat is improved during post mortem ageing. Stanton and Light (1987) have presented data which proved that perimysial collagen is damaged and partially solubilised during conditioning. Lewis *et al.,* (1991) revealed that the braking strength of the perimysial connective tissue in raw beef decreases during postmortem aging.
The weakening mechanism in intramuscular connective tissue is not known. Some components in ECM are degraded by metalloproteinases and lysosomal enzymes *in vitro* (Bailey and Light, 1989). But it is not clear whether the extracellular matrix in muscle is degraded by these enzymes during post mortem aging. PGs are degraded by β- glucuronidase which is released from the lysosomes in postmortem muscle (Møller *et al*., 1976). The activity of free β- glucuronidase increases with the postmortem aging, concomitant with the increase in the tenderness of beef (Dutson and Lawrie, 1974). Nishimura *et al.* (1996) have shown that the amount of PGs in bovine semitendinosus muscle decrease with time postmortem, and that

collagen fibril – associated PGs in the perimysium mostly disappear during postmortem aging of beef.

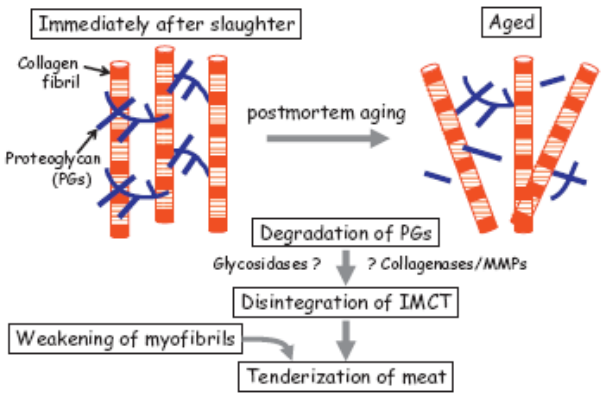

Figure 13: Schematic representation of changes in intramuscular connective tissue during post mortem aging. In muscle immediately after slaughter proteoglycans (PGs) link collagen fibrils and stabilize the intramuscular connective tissue. During post mortem aging, PGs are degraded and the linkage between collagen fibrils is weakened. This structural change in the intramuscular connective tissue contributes to the tenderization of aged meat (Nishimura, T., 2010).

2.4 Infrared spectroscopy

Infrared spectroscopy is a spectroscopic technique. The infrared region (figure 14) is located between the visible light, and the microwaves region. The infrared spectral region is from 750 nm to about 10000 nm. It can be further subdivided into the near-infrared region (750-2500nm), the mid-infrared region (2500-5000 nm) and to the far-infrared region (5000-10000nm) (Barth, A. 2007).

The position of an absorption band in the spectrum can be expressed in nanometers (nm), but the most common is wave number, which is proportional to the transition energy and frequency of absorbed light and has the unit cm^{-1} (Williams, D and Fleming, I, 2008, p 27).

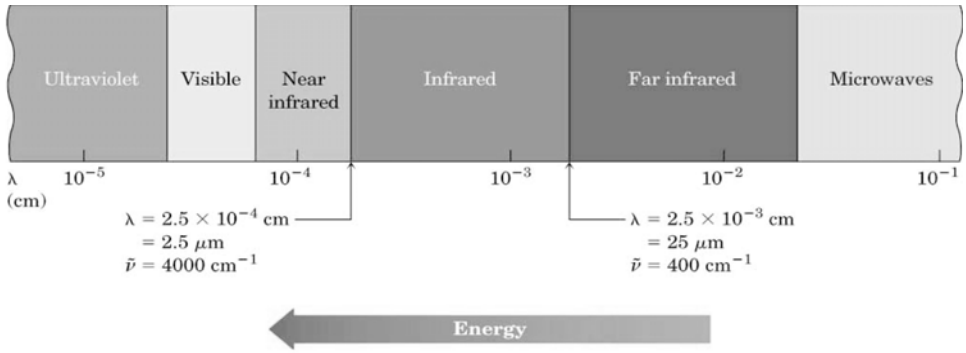

Figure 14: The electromagnetic spectrum. The infrared region is between the visible and microwave region.

The infrared spectra are associated with transitions between vibrational energy levels. A molecule absorbs only selected frequencies of infrared radiation. The probability of absorption and vibration frequencies depends on the strength and polarity of the vibration bonds which are influenced by intra- and intermolecular effects. The approximately position of an infrared absorption band is determined by the vibrating masses and the type of bond (single, double, triple), while the exact position is given by electron withdrawing or donating effects of the environment and by coupling with other vibration. The strength of absorption increases with increasing polarity of the vibrating bonds (Barth, A. 2007).
Not all the bonds are capable of absorbing infrared energy; the bonds have to have a dipole moment that changes as a function of time. Bonds that are symmetric, like H_2 or Cl_2 do not absorb infrared radiation. The bonds have to present an electrical dipole that is changing at the same frequency as the incoming radiation in order for energy to be transferred (Pavia *et al*. 2001 p.15).
Information that can be derived from the infrared spectrum

- Chemical structure of the vibrating group:

The molecules chemical structure is the dominating effect that determines vibrational frequencies via the strength of the vibrating bonds and the masses of the vibrating atoms. Changes in chemical structures can be detected (Barth, A. 2007).

- Chemical properties of neighboring groups in a molecule:

The electron density of a given bond in a molecule is influenced by neighboring groups within a molecule via inductive and mesomeric effects. Because of this the amide groups absorbing at lower wave numbers than the carbonyl groups of carboxylic acid (Colthup, *et al.,* 1975).

- Bond angle and conformation:

In a molecule vibrations in adjacent parts are often coupled. This coupling depends on details of the molecular geometry. Coupling can therefore provide insight into three-dimensional structure of molecules (Barth, A. 2007). An example is the transition dipole coupling of the C=O stretch bond in proteins (Socrates, G.2001)

- Hydrogen bonding:

The strength of hydrogen bond can be detected by vibrational spectroscopy. Hydrogen bonds stabilize the protein structure and it is essential for catalysis. Hydrogen bonding lowers the frequency of stretching vibration, since it lowers the restoring force, but increases the frequency of bending vibration since it produces an additional restoring force (Colthup, *et al.,* 1975).

When a sample absorbs infrared light, the energy of absorbed light is converted into atomic bond vibration. The vibration is either classified as stretching or bending. The stretching vibrations are classified to be either asymmetrical (movement in opposite direction) or symmetrical (movement in same direction). The bending vibration is classified as scissoring, rocking, twisting and wagging. See figure under.

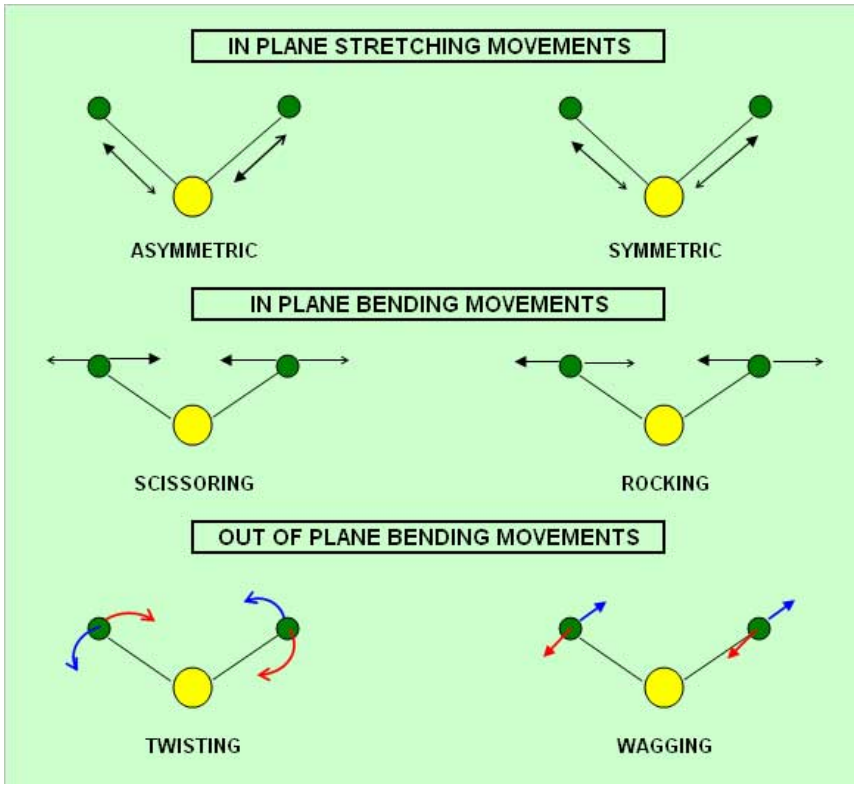

Figure 15: Different types of atomic vibration that can occur. (http://www.ptli.com/testlopedia/tests/FTIR-E168andE1252-more.asp)

An infrared spectrum has high information content that makes it a valuable tool to investigate protein structure of the molecular mechanism of protein reaction and of protein folding, unfolding and misfolding (Barth, A. 2007).

An IR spectrum on a large molecule can be composed of many overlapping bands with the consequence that much information can be hidden under broad, featureless absorption bands. To discover this information one can take the 2^{nd} derivative of the spectrum. By applying the derivation (DeNoyer and Dodd, 2002) spectral resolution can be enhanced and underlying features can be resolved facilitating the identification of existing structural motifs. In a 2^{nd} derivative a negative band with the minimum at the same wavelength as the maximum on the zero-order band. It also shows two additional positive satellite bands either side of the main band (Owen, A 1995). Underlying bands that is not visible in the original absorbance spectrum is uncovered by using the algorithm by Savitzky-Golay (Savitzky and Golay, 1964).

A typical example of an IR spectrum and the 2nd derivative collected from a single myofiber is shown in the figure under.

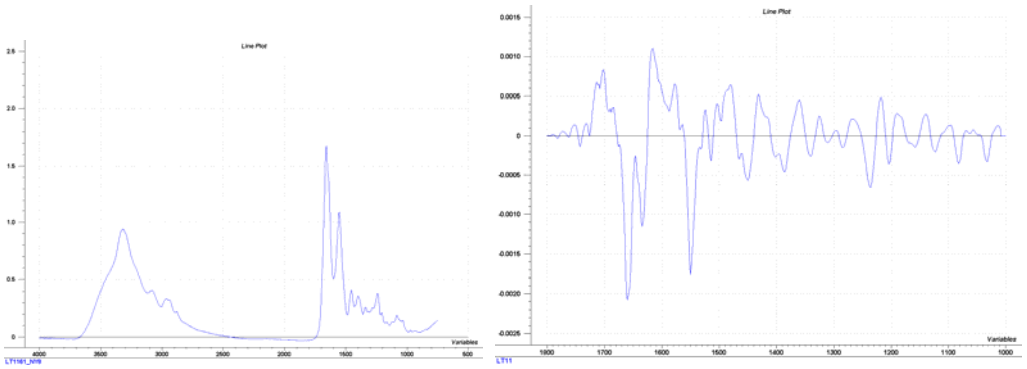

Figure 16: Shows an example of an IR spectrum and the 2nd derivative from 1800-1000 cm-1.

In the figure under, five of the nine amide IR modes that are typical for protein and peptides are showed. Origins of these bands are the amide group found in the protein backbone.

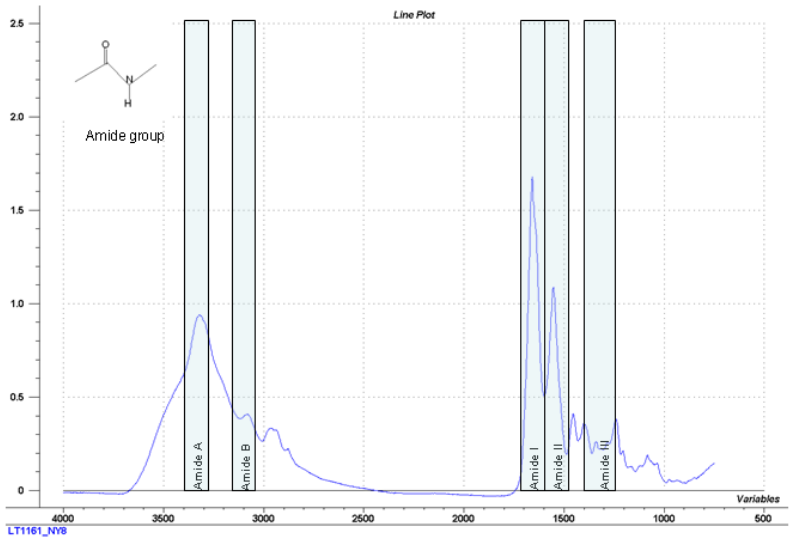

Figure 17: Spectrum of a single myofiber, the five amide modes that are typical for protein and peptides is indicated in light blue.

Amide A and B (~3300 and ~3070 cm^{-1})

N-H stretching vibrations give rise to the amide A band between 3310 and 3270 cm^{-1}. It is exclusively caused by the N-H group which is hydrogen-bonded, and is insensitive to the conformation of the polypeptide backbone of proteins. Its frequency depends on the strength of the hydrogen bond. The amide B bond between 3100 and 3030 cm^{-1} is due to Fermi resonance of the N-H stretching vibration with an overtone of the amide II vibration (Stuart, 1997).

Amide I (~1650 cm^{-1})

The amide I vibration, lying near 1650 cm^{-1}, arises mainly from the C=O stretching vibrations with minor contributions from the out-of-face C-N stretching vibration, C-C-N deformation and the N-H in-plane bend. The amide I vibration is only slightly affected by the nature of side chain.

The amide I band of polypeptides has for a long time been acknowledges to be sensitive to secondary structure. This has encouraged an interest in understanding the relationship between structure and spectrum. The amide I absorption depends on the backbone structure. The exact frequency of the amide I and II absorptions is influenced by the strength of any hydrogen bonds involving amide C=O and N-H groups.

In proteins the amide group is involved in a secondary structure of some type: either a helix or in an extended sheet. The characteristic frequencies for different secondary structures are often explained on the differences in their hydrogen bonding pattern. The dihedral angle can determine the chain geometry. The secondary structure is influenced by the length and direction of hydrogen bonds involving amide C=O and N-H groups. The variation in the length and direction of hydrogen bonds result in variation in the strength of the hydrogen bond for different secondary structures, which in turn produces characteristic electron densities in the amide C=O groups, which give the characteristic amide I frequencies. The stronger the hydrogen bond involving the amide C=O, the lower the electron density in the C=O group and the lower the amide I absorption appear. This approach can indicate that the lowest amide I frequency occur for extended polypeptide chains such as those found in denaturated proteins

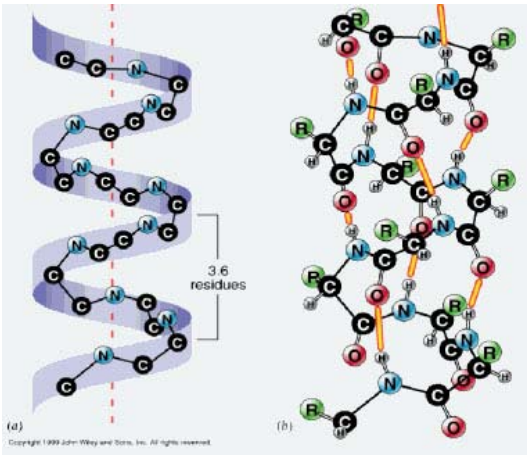

Figure 18: α-helix (http://www.uic.edu/classes/bios/bios100/lectf03am/lect02.htm)

A further band found in the amide I region occurring at 1666 to1670 cm^{-1} is discussed to be derived from C=O groups that are not involved in H-bonds, but in weak dipole-dipole interaction between the amide C=O and solvent S=O groups (Jacksen and Mantsch, 1995).

Amide II (~1550 cm^{-1})

The amide II band, absorbing around 1550 cm^{-1} is generated from out-of plane combination of the N-H in plane bend and the C-N stretching vibration with smaller contribution from the C-O in plane bend and the C-C and the N-C stretching vibration. The amide II vibration is also hardly affected by the side chain vibration. The correlation between protein secondary structure and frequency is less straight forward than for the amide I vibration. Nevertheless it provides valuable structural information and secondary structure prediction can be done with the amide II band alone (Barth, A. 2007).

Amide III (1400-1200 cm^{-1})

The amide III band is a combination of the in-phase N-H bending and C-N stretching, with small contribution from the C-O in plane bending and the C-C stretching vibration (Barth, A. 2007). In addition, often significant contribution of the CH_2 wagging vibration of amino acid chain can occur, which make interpretation of this mode complex (Krimm and Bandekar, 1986).

2.4.1 Fourier transforms infrared spectrometers

The name *Fourier transforms infrared (FTIR) spectrometers* originates from the fact that the detector signal of these spectrometers is related to Fourier transformation to the measured spectrum. A Fourier transform spectrometer performs two Fourier transformations, one by the interferometer and one by the computer. The interferometer is the heart of the FTIR spectrometer; it has a fixed and a movable mirror. The latter generates a variable optical path difference between two beams which gives a detector signal that contains the spectral information. Light emitted from the light source is split by a beam splitter, where about half of it is reflected towards the fixed mirror and from there reflected back towards the beamsplitter where about 50 % passes to reach the detector. The other half of the initial light intensity passes the beam splitter on its first encounter, is reflected by the movable mirror back to the beamsplitter where 50% of it is reflected towards the detector. When the two beams recombine they interfere and there will be constructive or destructive interference depending on the optical path difference *d*. The instrument measures the light intensity relative to the position of the movable mirror and this is called an interferogram. It turns out that the interferogram is the Fourier transform of the spectrum. A second Fourier transform performed by a computer converts the measured data back into a spectrum (Barth, A. 2007). In a sample measured in transmission mode, the infrared light passes a slide containing the sample before it reaches the detector. The sample absorbs light according to the Beer-Lamberts law:

$A = \log (I_0/I)$

Where A is the absorbance, I_0 is the light intensity before the sample and I the light intensity after the sample. Different slides are used, but the most common is ZeSe, BaF_2 CaF_2.

The figure 19 show a scheme of a FTIR spectrometer.

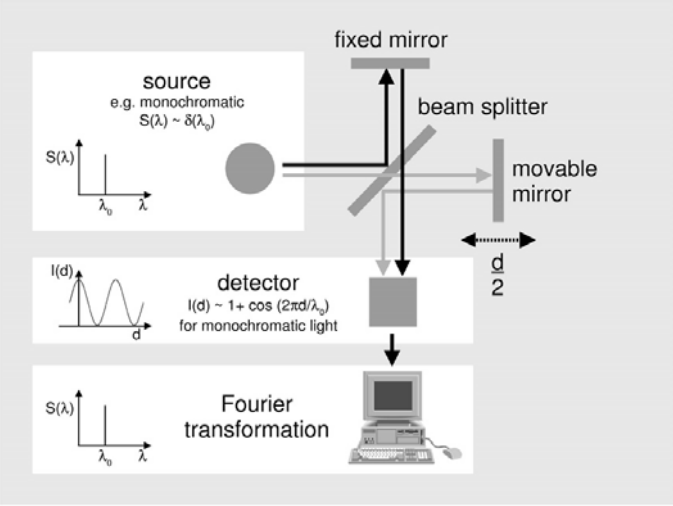

Figure 19: Scheme of a Fourier transform infrared spectrometer. The spectrum S (λ) is described by a delta function located at λ_0. Depending on the position of the movable mirror one obtains constructive or destructive interference at the detector and the detector signal I (d) varies as a cosine function with the mirror position which determines the optical path difference d. The cosine and the delta function describing the monochromatic spectrum are related by a Fourier transformation. The spectrum S (λ) is performed by a second Fourier transformation by a computer (Barth, A. 2007).

2.4.2 Fourier transform micro spectroscopy

Fourier transform (FT)-IR micro spectroscopy is a combination of spectroscopy and microscopy. It is a powerful technique used in biological science to study the biochemical composition of microscopic tissue sections. The big advantage of this technique is that the sample preparation is easy and the acquisition is fast. There is no need for any staining, which also allows only one single or just a few components to be analyzed. FTIR microscopy gives an overall chemical fingerprint with more or less detailed information about several macromolecules. The challenge of FTIR microscopy is to treat the huge amount of data and information you get. A single FTIR image contains many image point (pixels) with a full spectrum with up to several thousand wave numbers in every pixel point. The data analysis of a set of FTIR images faces many important data analytical problems (Kohler *et al.,* 2007):

1. Quality differences: the quality of the spectra can vary according to quality differences of detector pixels, due to regions with low intensities and due to scatter

effects like surface effects on tissue section and differences in the optical path length. This make a filtering of spectra including pre-selection and pre-processing very important (Kohler *et al*. 2005 and Martens *et al*. 2003).

2. Spatial variation in tissue: the FTIR tissue image may contain information from more than one tissue type and there are local spatial variations in every tissue type (Kohler *et al.,* 2007).
3. Inhomogeneous images: when investigating sets of inhomogeneous images every image have to correspond to certain sample information or to certain design variables. An analysis that involves both design/sample information, characterizing of every single image and spatial variation that considerate the inhomogeneous within every image is needed. To make the images comparable is requires stable models for standardization of images. Other parameters that can vary within and between the images are the intensity of the light source and sample thickness (Kohler *et al.,* 2007).

2.4.3 Extended multiplicative signal correction

To interpret the spectra it is important to separate the physical information like scatter effects due to differences in the effective optical path length, due to variation in the light source or due to other effects like surface effects of the sample from the chemical information originating from the samples. To separate this information a model-based-preprocessing method like mulitiplicative signal correction (MSC) and extended mulitiplicative signal correction (EMSC) can be used. In a basic form of EMSC every spectrum $z(\tilde{\nu})$ is a function of the wave number $\tilde{\nu}$, which is defined as the reciprocal of the wavelength λ. The spectrum $z(\tilde{\nu})$ can be written as

$$z(\tilde{\nu}) = a + b \cdot m(\tilde{\nu}) + d\tilde{\nu} + e\tilde{\nu}^2 + \varepsilon(\tilde{\nu}) \qquad (1)$$

a linear combination of a baseline shift a, a multiplicative effect b times a reference spectrum $m(\tilde{\nu})$, linear and quadratic wave number- dependent effects $d \cdot \tilde{\nu}$ and $e\tilde{\nu}^2$, respectively. The term $\varepsilon(\tilde{\nu})$ contains the unmodelled residuals. The reference spectrum $m(\tilde{\nu})$ is calculated by taking the sample mean of the considered set of spectra or by selecting a spectrum from the sample set as reference spectrum (Kohler *et al.,* 2007).

The EMSC parameters a, b, d and e can be estimated by ordinary least-squares, and finally the spectra can be corrected according to

$z_{corr}(\tilde{\nu}) = (z - a - d\tilde{\nu} - e\tilde{\nu}^2)/ b$ (2)

The EMSC model only account for scatter effects and does not use constituent difference spectra (Kohler *et al.,* 2005).

The EMSC model is defined around a reference spectrum which makes it very stable, even in the case where there are very strong spectral changes (Kohler *et al.,*. 2007).

The EMSC can also estimate the scatter effects, the obtained scatter effect can therefore be visualized in the same way as the chemical properties (Kohler *et al.,*. 2005).

2.4.4 Polarization imaging

With polarized light microscopy the orientation of chemical bonds can be investigated. The frequency at which a molecule absorbs polarized can be used to obtain information about the orientation of specific bonds. The orientation of collagen molecules has been investigated in a semi-quantitative fashion in articular cartilage by polarized Fourier transform infrared imaging spectroscopy (Camacho *et al*. 2001). This analysis was based on changes in the integrated areas of the collagen amide I and amide II vibration (Bi. *et al.* 2005).The ratio of the integrated PG/ Amide I can indicate the quantity of PGs present. The areas are shown in figure 20.

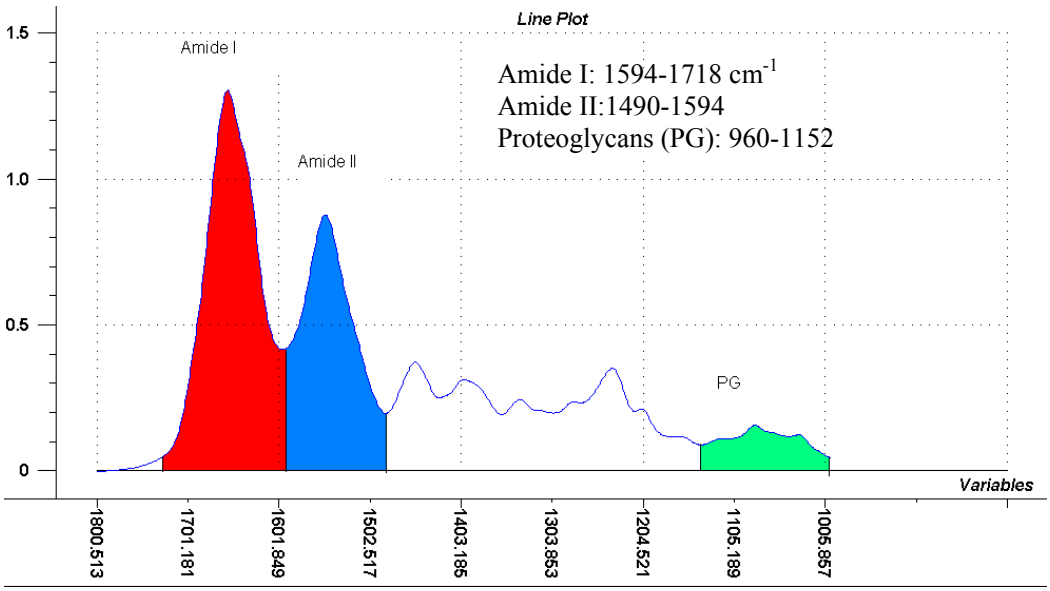

Figure 20: The areas which are integrated to indicate the orientation and quantity present of collagen and Proteoglycans.

Bi *et al.* (2005) has tried to establish a reliable method that can be used to determine the alignment of collagen molecules in cartilage by FT-IRIS more quantitatively. A reference like this would have advantages over current techniques of elucidating changes in collagen orientation based on changes in molecular interaction. To calibrate the spectral parameters highly oriented tendon collagen (type I) was used. This data was applied to FT-IRIS analysis of the orientation of collagen molecules in three types of cartilage tissue to demonstrate that the FT-IRIS method of determining collagen orientation is valid in tissues with different pathologies; normal equine articular cartilage, a tissue with known zonal variation in collagen orientation, equine cartilage repair tissue, and human osteoarthritic tibial plateau cartilage. During the study polarized FT-IRIS data were acquired from tendon at different angles.
The result of this study shows a sinusoidal variation for both amide I and amide II peaks area based on their dichroism. With a polarization angle between 0 º and 20 º the amide I area was maximal and the amide II area was minimal. The amide I/II peak ratio varied also sinusoidally, with the magnitude of amide I /II ratio ranging from 4.1 to 0.9, with the maximum occurring with polarization angle at ~ 15 º, and the minimum at polarization angle at ~ 100 º.

3 Material and methods

3.1 Sampling

Bovin *M. psoas major* (PM) and *M. semitendinosus* (ST) were subjected from the same animal 3 days post mortem. Both left and the right muscle from the animal were used in this experiment.

The muscle was stored at 4 º C for 3, 7, 11, 15 and 19 days.

Figure 21: Shows the muscles, M. semitendinosus (ST) to the left and M. psoas major (PM) to the right.

From each muscle a 3, 5 cm thick slice was cut. The left part was used for tenderness measurement with Warner Bratzler sheer force and the right part for biochemical, FTIR and histology analyses. After each day the rest of the muscle was vacuum-packed and stored at 4 ºC until the next trial day.

Figure 22: Shows a 3, 5 cm thick slice of the muscles, M. semitendinosus (ST) to the left and M. psoas major (PM) to the right.

3.2 Textural measurement:

The samples were vacuum-packed in polyethylene bags and heat-treated in a water baths at 70 ºC for 50 min and cooled in ice water for 50 min. After the treatment the sample were unpacked to take away the water loss, and vacuum-packed again. The sample was stored in the fridge until the next day. Before the Warner Bratzler sheer force measurement the temperature of the samples was stabilized for 1 h at 20 ºC. From the piece of muscle slices with the size 1 x 1 x 2 cm were cut along the fibre direction of the muscle to give the final samples cross-section dimensions. Structures with visible fat were avoided. The textural properties were studied by measuring the force needed to cut the samples at right angles to the myofibrils. For the measurements a WB shear press device called Instron Testing Machine (model 4202, Instron Engineering Co., High Wycombe, U.K.) was used. The average of the maximum force of 10 measurements from each meat sample was used to calculate the tenderness in the samples.

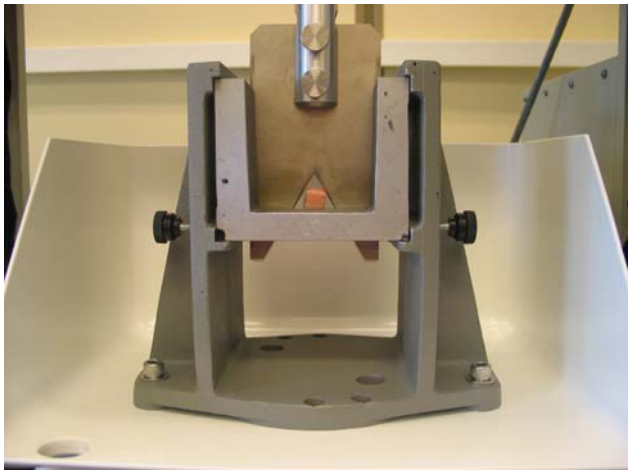

Figure 23: Warner Bratzler sheer force measurement.

3.3 FT-IR and histology preparation

Blocks for FTIR and histology analysis where prepared from different location of the muscle. The remaining part was stored at -80 ºC for biochemical analysis.

From these blocks samples were cut into small pieces of approximately 0, 5 x 0, 5 x 0, 3 mm along the fibre direction and embedded in optimal cutting temperature (OCT) compound

(Tissue-Tek, Sakura Finetek, USA) and frozen immediately in liquid nitrogen. OCT was used to avoid freezing damage of the sample. Until sectioning the samples were stored at - 80 ºC.

Figure 24: left: samples for FTIR and histology covered with O.C.T. compound. Right: Samples has been frozen in liquid nitrogen.

8 µm muscle cross-sections were cut in a cryosat (Leica CM 3050 S, Nussloch, Germany) at – 22 ºC. Sections were subjected in parallel for FT-IR analysis and histological analysis. The samples were sections transversally to the fibres direction. The tissue blocks were unfixed and there was no need of chemicals to achieve signal detection. The only alteration taking place is caused by desiccation of the tissue. Sections were prepared and thaw-mounted on infrared-transparent 2 mm-thick ZeSe slides for FT-IR microscopic measurements. The slides were stored in an exsiccator until measuring. For the histological samples the 8 µm thick sections were prepared. The microscope slides were stored in -20 ºC until staining.

3.4 Biochemical analysis

Muscles pieces were powdered in liquid nitrogen. The muscles were cut in small pieces and frozen in liquid nitrogen. The frozen pieces were putted into Ika Universallmühle (Janke & Kunkel, Gmbh, Ika labortecnic Staufen, Germany) shown in figure to the left to be powdered.

The frozen powder were immediately frozen in – 80 until further analysis.

The concentrations of sulphated GAGs in the muscles were measured using the Blyscan assey, according to the manufacture's protocol (Biocolor Ltd. Northern Ireland).
5.0 g of frozen meat powder were putted in 40 ml papainbuffer (0,1M Tris HCl pH =7, 4, 0.005 M cystein). The amount of papain was 250µl of 50mg papain/ 1Ml d H_2O. The solution was incubated for 24 h at 37 ºC for papain digerering..
Then the solution was centrifuge at 12 000 rpm for 30 min at 4 ºC. The volume of the extract was measured.
Because of the low level of GAGs in the muscle, the extract had to be "up concentrated" by ethanol. This was performed on all samples in order to be able to compare the samples.

A precipitate was formed by binding of the Blyscan dye to free GAGs or GAGs linked to protein core remaining after the papain digestion. After dissociation of the precipitate compelx, the GAG concentration was determined photometrically using the corresponding calibration curve.

3.5 Fourier-transform infrared micro spectroscopy

Single element spectra
An optical IR spotlight 400 microscope (Perkin Elmer) coupled to a Spectrum 400 FT-IR spectrometer (Perkin Elmer, UK) was used to measure the tissue sections. The microscope has a moving stage for sample scanning and a liquid nitrogen cooled 16-element MCT (mercuric cadmium telluride) detector. The movement precision of the stage is 1 µm. The microscope also has a visible light source to focus the sample and to define/choose the region of interest for infrared measurement.
IR spectra were collected from connective tissue regions in transmission mode from 4000 to 650cm^{-1} with a spectral resolution of 8 $cm^{-1,}$ 64 scans per pixel and with spectral interval of 4 cm^{-1}. A background spectrum of the ZeSe substrate was recorded before each sample measurements in order to account for variation in water vapour and CO_2 level. To compensate for influence of water vapour and CO_2, measurements was carried out in a closed compartment flushed by dry air.

Polarized image

Polarization experiments were performed to determine the spatial distribution of the collagen orientation in the different muscles and during storage. A spectrum Spotlight FTIR imaging system (Perkin Elmer, Bucks, UK) were used.

This system consist of an Spectrum 400 FT-IR spectrometer coupled to an optical IR spotlight 400 microscope with a 16 x 1 linear array of detector elements which has the capability to image a rectangular sample size up to several millimetres in length at a spatial resolution of 6,25 μm.

Polarization data was acquired by placement of a polarization filter between the sample and the impinging IR radiation in the spectrometer. The IR dichroic ratio of amide vibration, R, has been used as an indicator of orientation of the secondary structure of protein and peptides. R is defined as the ratio of absorbance for one component under parallel polarized light ($A_{\parallel}$) and perpendicular ($A_{\perp}$). IR spectra is collected using two polarizations, θ = "0" and θ = "90" addition to non-polarized. At angle "0" the strongest absorbance will be from bonds vibrating along the y axis. When the polarizer is at "90", the strongest absorbance will be from bonds vibrating along the x axis. (fig 25) (Bi *et al.,* 2005). If the collagen fibrils in the sample have no overall orientation, it is expected to see the same intensities in the "0" and "90" images. The ratioed image would show "1" for all the values. If the collagen fibrils are parallel to the x axis in the samples, then the amide I vibration moment is perpendicular to the x axis, or, along the y axis, and you would have a maximum intensity in the "0" image, and a minimum intensity in the "90" image. In the ratioed images, where the values are greater than 1, it indicates some collagen fibril orientation along the x axis. Where the values is less than 1 indicates some collagen fibril orientation along the y axis.

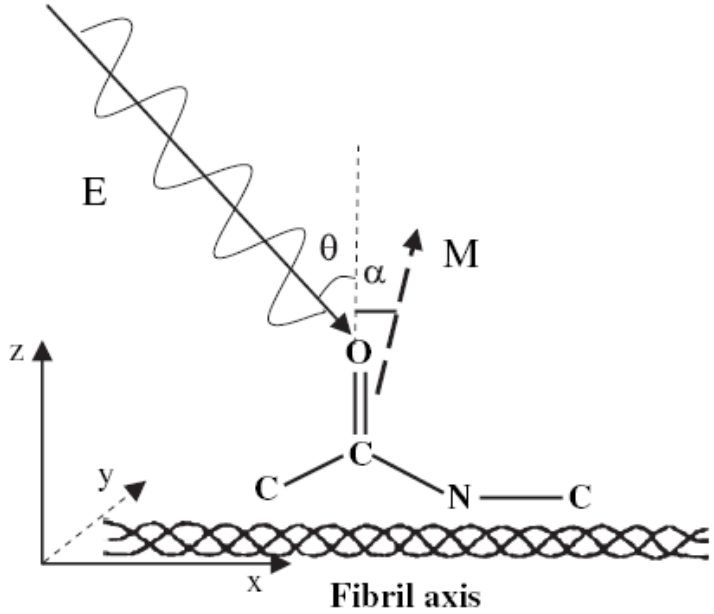

Figure 25: Schematic of the collagen fibril and the incidental polarized light (E, θ degrees) absorbed by the amide group. The transition moment of the amide I vibration (M) is at an angle approximately 0 º with the fibril orientation normal (α). θ: Angle of polarization; α: angle between amide I transition moment and fibril orientation normal; z-axis: θ = 0 º; x-axis θ = 90 º.

The (primary) macromolecular components of connective tissue, collagen and PG give rise to specific absorbance band in the infrared.

Integrated absorbance band area were calculated and utilized as indicators of the quantity of component present. Collagen was monitored in the 1590-1720 cm^{-1} spectral region (amide I absorbance). Proteoglycans (macromolecules consisting of sulphated GAGs linked to a core protein) in the 985 – 1140 cm^{-1} spectral region. Absorbances in this region arise from vibration of the C - O – C and C – OH bonds.

The relative quantity and distribution of proteoglycans were calculated with the ratio of the integrated areas of the PG absorbance to the aminde I collagen absorbance. The calculated content was compared to histological data and biochemical data (Kim *et al.*, 2005)

The polarizer was rotated and the tissue sample was at the same position to ensure the same tissue region was consistently sampled.

Data were analysed with Matlab v 7.10 with some in-house routines made by Achim Kohler.

3.6 Histological Analysis

Alcian blue staining.

To outline the connective tissue and monitor the presences of sulphated glycosaminoglycans, Alcian Blue- stained sections from the same tissues utilized for FTIR analyses were examined by light microscopy. Alcian blue 8GX (Gurr Biological Stains, BDH, Poole, UK), 0.05 % in 0.2 M Na-acetate buffer, pH 5.8, with 0.06 and 0.4 M $MgCl_2$, was used as staining solution. At a concentrate of 0.06 M $MgCl_2$, all anionic groups in the material are stained. By increasing the $MgCl_2$ concentration to 0.4M, only negatively charged groups such as sulphated proteoglycans are stained (Scott and Dorling, 1965). The section were immersed in staining solution at room temperature with gentle shaking overnight, rinsed in running water , dehydrated in absolute ethanol, cleared in xylene and mounted in Eukitt.

There can be variations of sample thickness, even though all section were cut at a set thickness of 8 μm, the actual thickness of the section can vary by 20 % (Kim, M. et al. 2005) due to inherent limitation in the precision of the cryostat. The challenge with Alcian blue methods that the staining intensity is very pH dependent, and also varies with the concentration of ions used in the staining solution (Ippolito, E et al., 1983). To minimize these effects the tissue sections of the two muscles were stained at the same time and the pH of the solution were adjusted accurately.

Collagen I staining.

The procedure for the collagen I staining is described under. In the staining there is a used antibody which binds to epitopes in collagen I in the connective tissue. The analyze kit is called: DakoCytomation EnVision+System-HRP (DAB), For use with Rabbit Primary Antibodies Code K4010. The staining was done according to the protocol that followed the kit, except that the incubation time with Peroxidase Block was extended to 3 h and 45 min.

4 Results

4.1 Textural measurement:

The two muscles showed various results regard to tenderness. The WB-value of ST was higher than the WB-value of PM at 3 days post mortem, indicating the ST muscle to be tougher. Both muscles showed a decrease in WB-value during storage 3, 7 and 11 days post mortem, reflecting a tenderization of both muscles. At 15 days post mortem they got similar values. A higher value was obtained after 19 days of ST muscle.

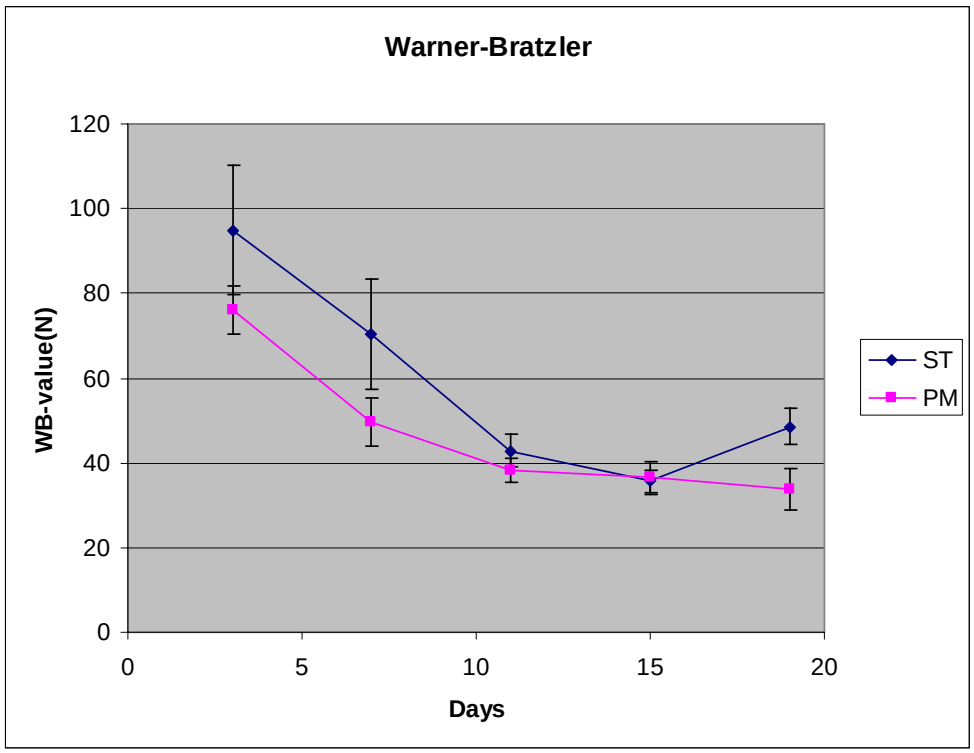

Figure 26: Shows the Warner-Bratzler results in the two muscles, M. semitendinosus (ST) and M. psoas major (PM).

4.2 FT-IR micro spectroscopy

Single element spectra were measured on connective tissue in the muscle. To resolve nearby lying bands in the spectra, the spectra were derivatised (second derivative) using the algorithm by Savitzky-Golay. The spectra were then pre-processed by EMSC.

Figure 27 shows the second derivative spectra for the 2 different muscles, ST (blue) and PM (red) at 3 days post mortem storage from 1800-1100 cm^{-1}. The minima in the second derivatives refer to the maxima (bands) in the original spectra.
The different peak absorbance's were selected in the region 1800-1000 cm^{-1} according to the minima in figure 27.

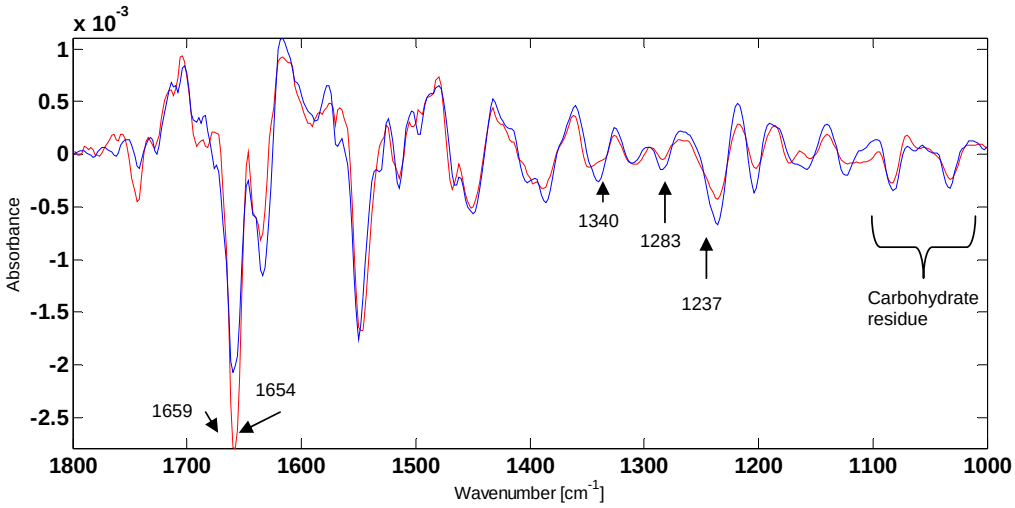

Figure 27: Mean second derivative spectra for PM (red) and ST (blue) at 3 days post mortem storage from 1800-1100 cm^{-1}. The minima in the second derivatives refer to the maxima (bands) in the original spectra.

Tentative band assignment made according to the literature are summarised in Table 2.

Table 2: Assignment of FTIR bands

FTIR Bands (cm^{-1})	Assigment	References:
1695, 1677	Amide I, Possible .reducible collagen cross-links (C=O stretch)	Miller et al. (2004), Paschalis et al. (2001) and Paschalis et al. (2003) and Camacho at al (2001)
1659	Amide I, Possible non-reducible collagen cross-links (C=O stretch)	Miller et al. (2004), Paschalis et al. (2001) and Paschalis et al. (2003) and Camacho at al (2001)
1652-1657	α - helix	Jackson and Mantsch (1995)
1340	CH_2 side chain vibration of collagen	Camacho at al (2001) Jackson et al (1995)
1283	Collagen Amide III vibration with significant mixing with CH_2 wagging vibration from the glycine backbone and proline sidechain	Jackson et al (1995)
1237	sulfat strech from proteoglycans, Collagen amide III vibration with significant mixing with CH_2 wagging vibration from the glycine backbone and proline sidechain.	Jackson et al (1995)
1083, 1062, 1031	C-O stretching vibration of the carbohydrates residues present in collagen and in proteoglycans.	Jackson et al (1995)

4.2.1 Collagen

The major feature in the spectra is the amide I absorption band (fig. 27) between 1610 -1690 cm^{-1} which arises from the stretching vibration of the proteins of the C=O groups of amide groups in proteins. The amide I absorption gives information of particular secondary structures within any one protein in IR spectra of tissue. The amide I absorption also give rise to non-protein components of tissues. The most intense non-protein absorption is most tissue arises from the O-H bending vibration of water (a band at around 1640 cm^{-1}).

In the amide I spectral peak there are two underlying bands that are of particular interest in the study of collagen: one at ~ 1660 cm^{-1} and one at ~1690 cm^{-1}. Figure 28 shows the 1660 band.. During collagen denaturation experiment, the relative intensity of the former decrease, while

the latter increase (Lazarev and Lazarev, 1978 and Lazarev *et al,.* 1985**)**. There is previously reported that the area ratio of these two bands (1660:1690) appears to correspond to the ratio of non-reducible/reducible collagen crosslinks in bone (Paschalis *et al,.* 1998). The spectra from PM muscle shows an decrease at the 1660 cm^{-1} from 3 to 15 days post mortem storage, except from 11 days post mortem. At 1690 cm^{-1} (result not shown) there is also a decrease in the spectra. In the ST muscle there is a decrease at 1660 cm^{-1} from 3 to 7 days post mortem storage, and then an increase to 11, 15 and 19 days post mortem storage. At 1690 cm^{-1} (result not shown) there is a decrease from 3 days post mortem to 7, 15, 11 and 19 days post mortem storage. No strong tendency due to collagen denaturation experiment mentioned above was obtained for the two muscles due to storage. The ratio of these 2 bands (1660:1690) in this experiment doesn't show any tendency about the non-reducible/reducible collagen crosslinks in tissue (result not shown), which further support this statement.

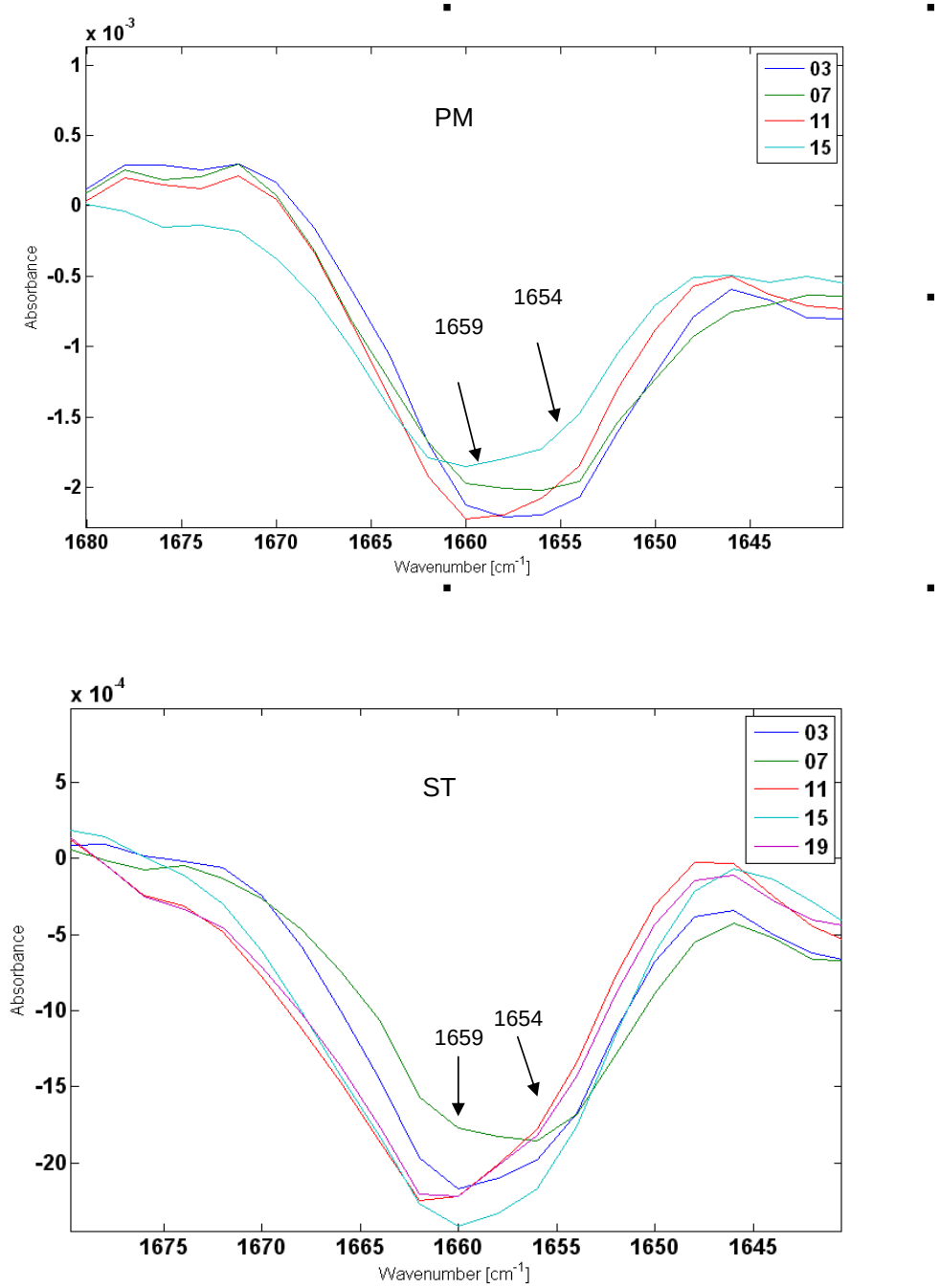

Figure 28: Amide I region (1610-1690 cm^{-1}): Possible non-reducible collagen cross-links (C=O stretch) and the absobance of α-helix 1654 cm^{-1} in PM (upper panel) and ST (lower panel).

However, if one considers just the band at 1659, which arises from possible non- reducible collagen cross-links (Miller et al. (2004), Paschalis et al. (2001) and Paschalis et al. (2003) and Camacho at al (2001)), the result from these spectra can indicate a reduction in non-reducible collagen cross-links in the PM muscle during storage from 3 to 15 days post mortem, with exception of 11 days post mortem. In the ST muscle the absorbance is more random obtained.

The absorbance between 1652 and 1657 cm^{-1} is accorded to the α-helix (Jackson and Mantsch. 1995). At 1654 cm^{-1} the PM muscle shows a decrease in the absorbance during aging time. The ST muscle has the same tendency, but it is not that clear as in PM. This can indicate a lower electron density in the C=O group and a decomposition of the α-helix.

The band at 1340 is discussed to be a marker for collagen (Camacho at al (2001) and Jackson et al (1995)).The figure 29 shows an increase in the absorption in both muscles due to storage. In the PM muscle there is a tendency in difference in collagen during storage, since the 3 and 7 days post mortem spectra are grouped together, and the 11 and 15 days post mortem spectra are grouped together. The differences between the absorbance in ST muscle are not that considerable.

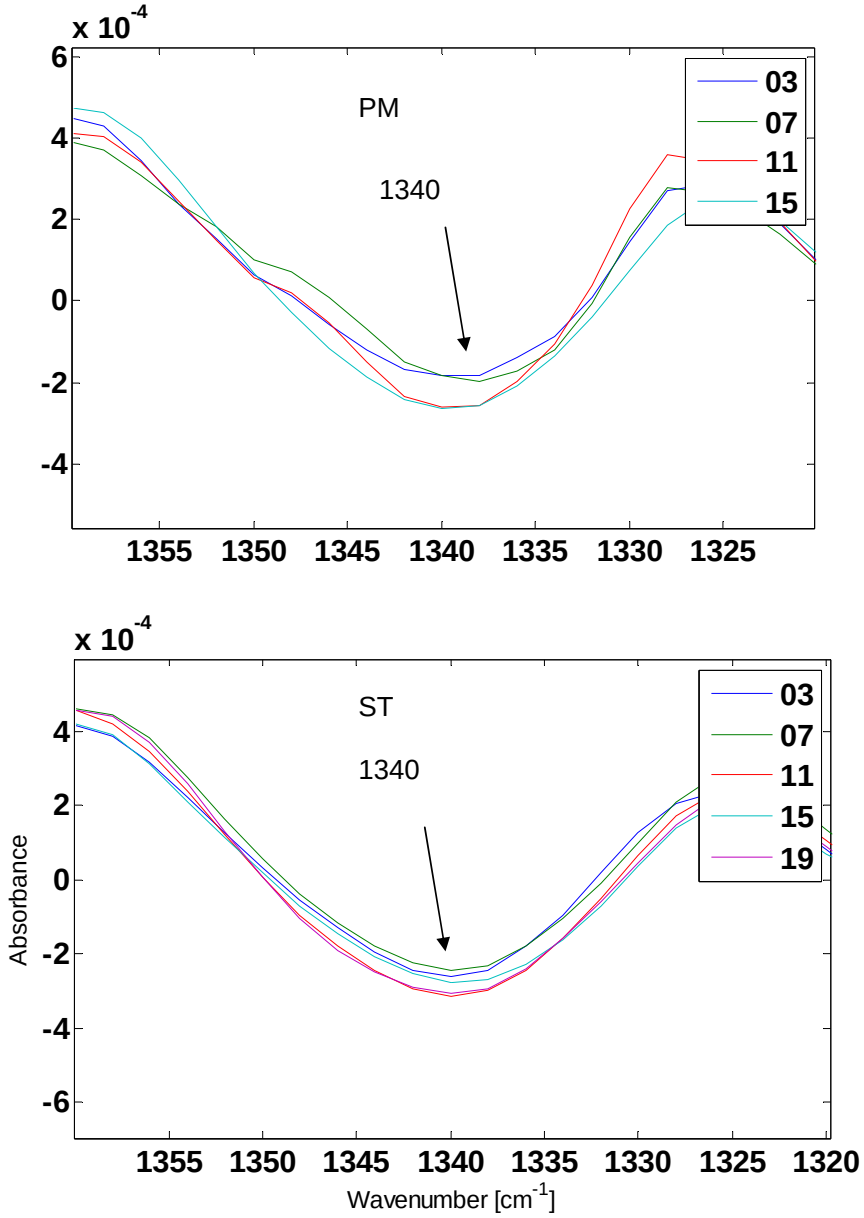

Figure 29: Shows the spectra from PM (upper panel) and ST (lower panel) at 1340 cm^{-1}. This band is discussed to be a marker for the integrity of collagen.

The high proportion of glycine and proline residues may give the characteristic spectrum between 1200 -1400 cm^{-1} in collagen. Absorption in this spectral region is generally attributed to the amide III.

The absorption at band 1282 cm^{-1} (Figure 30)of the PM muscle shows that 3, 7 and 11 days post mortem storage is grouped together, while the spectrum from 15 days post mortem has a higher absorbance. In the ST muscle one can see a clear grouping for the 3 and 7 days post mortem storage compare to the 11, 15 an 19 days post mortem storage which has a higher absorbance.

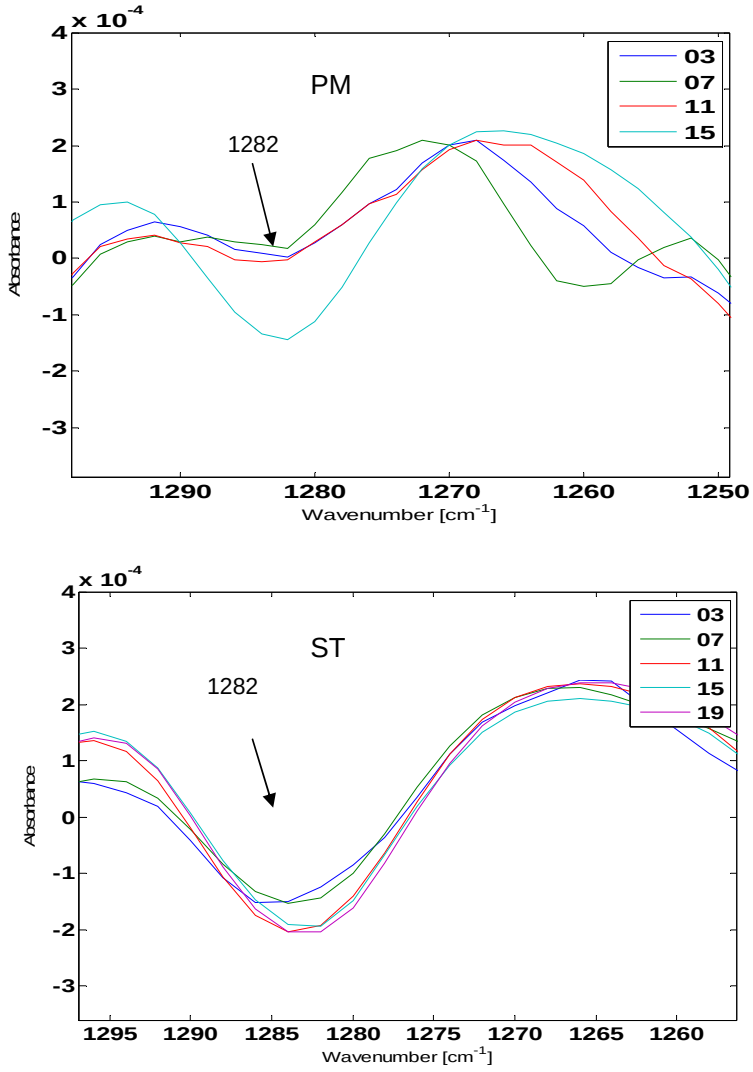

Figure 30: Shows the spectra from PM (left) and ST (right) at 1282 cm^{-1}.

To investigate the orientation of collagen the images were polarized with the angle 0º and 90º. To detect the connective tissue, the images were calculated at 1240 cm^{-1}. The spectra at 1240 cm^{-1} show that there are differences due to collagen content in the sample, and the FT-IRIS image shows the distribution of collagen. The red parts in figure 31 have high absorbance in the image correspond to high collagen content. The middle part shows a lower content of collagen, because it is also affected from the absorption from the fiber down in the marked area. The blue part is representing the fiber, which is low in collagen content. The FT-IRIS image is corresponding to the light microscopy image.

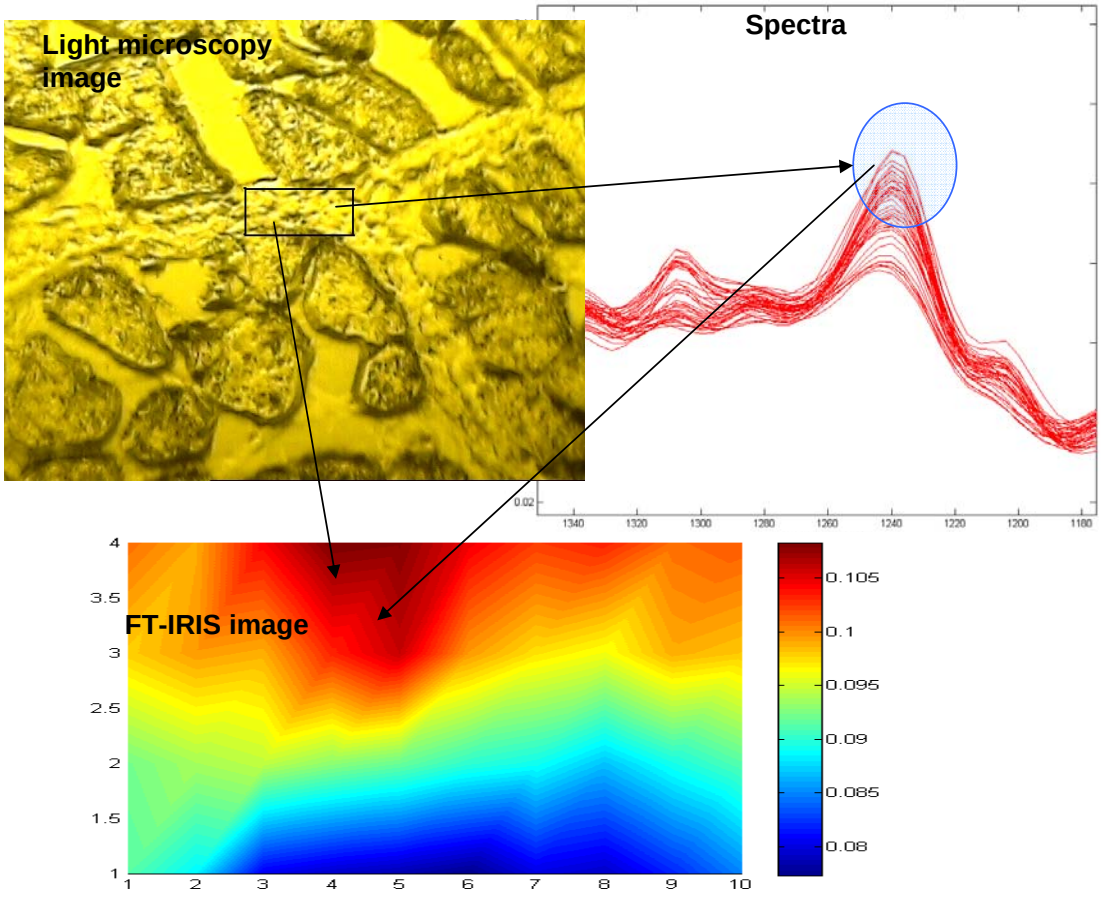

Figure 31: shows a visible image of the tissue section. The FT-IRIS image is taken in the marked region that contains connective tissue. The FT-IRIS image shows the absorbance at the marked area in the light microscopy image. The red parts with high absorbance in the image correspond to high collagen content

For polarized 4 picture were analysed, two from each muscle at different storing time.
PM muscle is analysed 3 and 7 days post mortem, while ST muscle is analysed 3 and 11 days post mortem.
To investigate the orientation of collagen, the sample was measured with two different polarization filters with the angles 0º and 90º. The ratio between amideI 0º / amideI 90º were imaged. Ratios greater than 1 indicate some orientation parallel to the x-axis. A ratio at 1 indicates no orientation, and ratio below 1 indicates some collagen fibril orientation along the y axis.
The images under shows the absorption at 1240 cm^{-1} to indicate the distribution of collagen in the sample, and the ratio amideI 0º / amideI 90º .
The PM muscle is showed under (Figure 32).

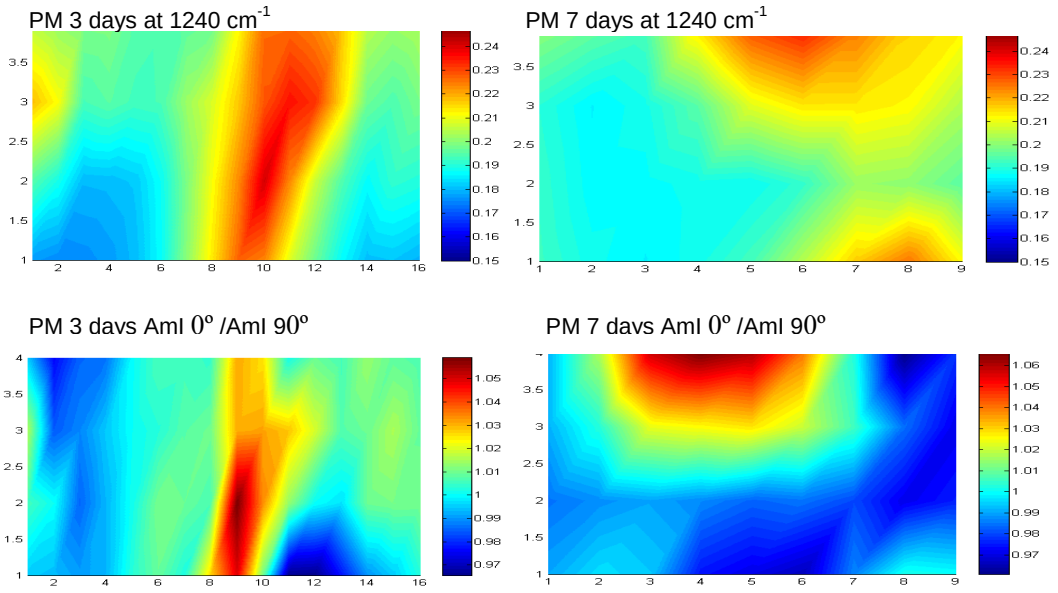

Figure 32: The images under shows the absorption at 1240 cm^{-1} to indicate the distribution of collagen in the sample. The ratio amideI 0º / amideI 90º is from 0.97 to 1.06, which indicates a random orientation

The ratio values range between 0.97-1.06, which is very close to 1 for both days. The collagen fibrils in the PM muscle is considered to be quite random oriented.

The ST muscle (Figure 33) is more heterogeneous, where the ratio value at day 3 post mortem is between 0.8 – 1.25. The areas with value higher than one indicate an orientation parallel to the x-axis. The ratio value at 11 days post mortem lower, it ranges from 0.98-1.03, these value are very close to 1, so one can assume that there has been a structural change in the ST muscle during storage.

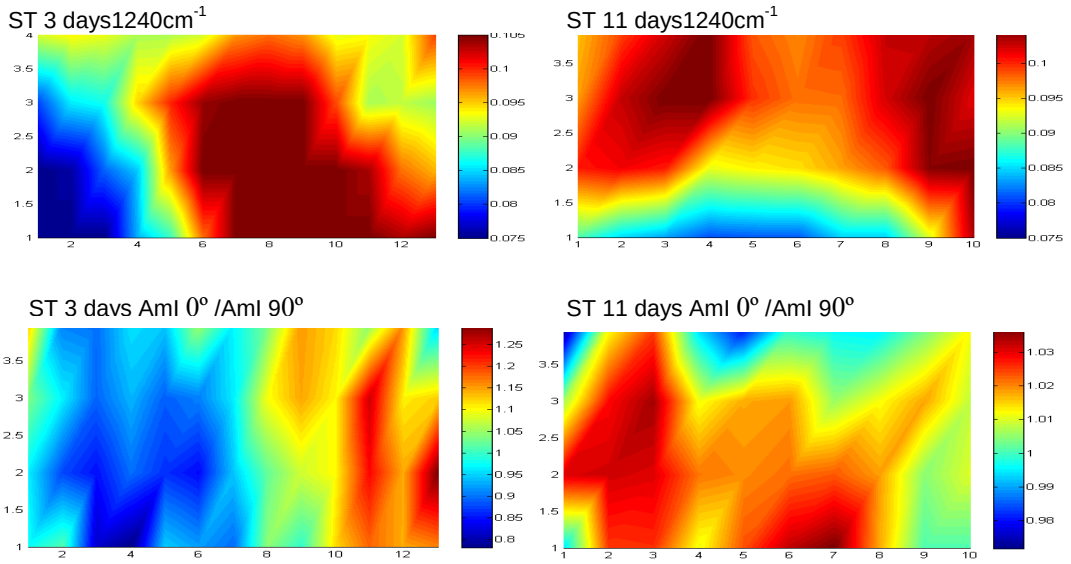

Figure 33: ST muscle at 3 and 11 days storage. At the top image at 1240 cm^{-1} show the collagen distribution. The images under shows the ratio between amideI/amideII at non-polarization angle and at polarization angle 0 and 90 º.

Tissues sections of PM and ST muscle were stained with antibodies against collagen I. In the figures below (Figure 34) one can clearly see collagen I staining in the perimysium as the most noticeable connective tissue, and in the epimysium which surrounds each muscle fiber. The distribution of the epitopes recognized by the antibody differed between the two muscles. The perimysium of ST muscle showed a wavy appearance with clear thread-like like structures, in contrast to PM which showed a more diffuse staining pattern of the perimysium.

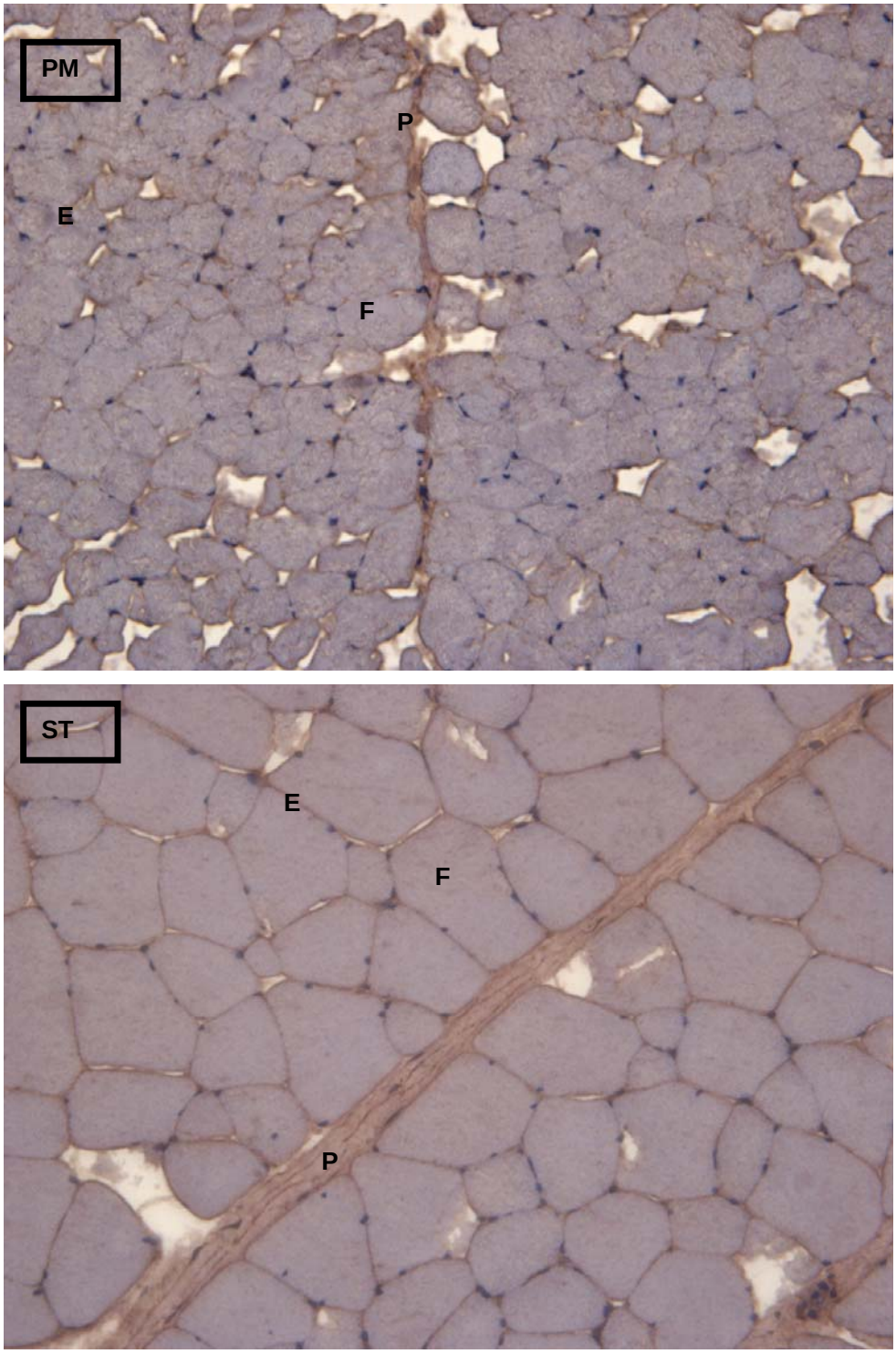

Figure 34: Collagen I staining of cross section of ST and PM. There is a clear difference in the size and structure of the perimysium. P= perimysium, F= fiber, E= epimysium

No clear differences in staining intensity, with more disintegrated areas not staining for collagen I could be detected between the two muscles or due to post mortem storage. Both muscles showed this intramuscular variance (Figure 35)

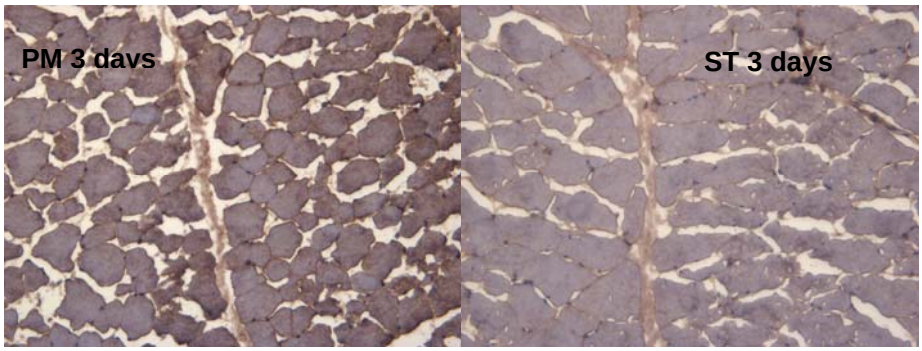

Figure 35: No clear differences in staining intensity could be detected between the two muscles or due to post mortem storage. Both muscles showed disintegrated areas not staining for collagen I, as illustrated in the figure. The differences in these images can also be due to the different quality of the sections.

4.2.2 Glycosaminoglycans (GAGs)

The amount of sulfated GAGs differed between ST and PM muscle, and also during storage post mortem. ST muscle contained more sulfated GAGs compared to PM. The decrease in GAG content during storage was more pronounced in ST compare to PM. The amount of sulfated GAGs in ST decreased from 373 µg/g to 210 µg/g in nitrogen powered material, and with biggest difference between 3 and 7 days post mortem. In PM muscle the amount varied from 170 to110 µg/g during the period, but with smaller differences in total amount during the storage period.

Some discrepancy in the GAG degradation pattern due to storage was also seen, mainly in PM muscle, with higher amount of GAGs at 7 days post mortem compared to 3 days post mortem. This discrepancy in GAG degradation pattern most likely is due to biological heterogeneity of connective tissue within the skeletal muscle. Loss of water could also explain this discrepancy in GAG degradation pattern.

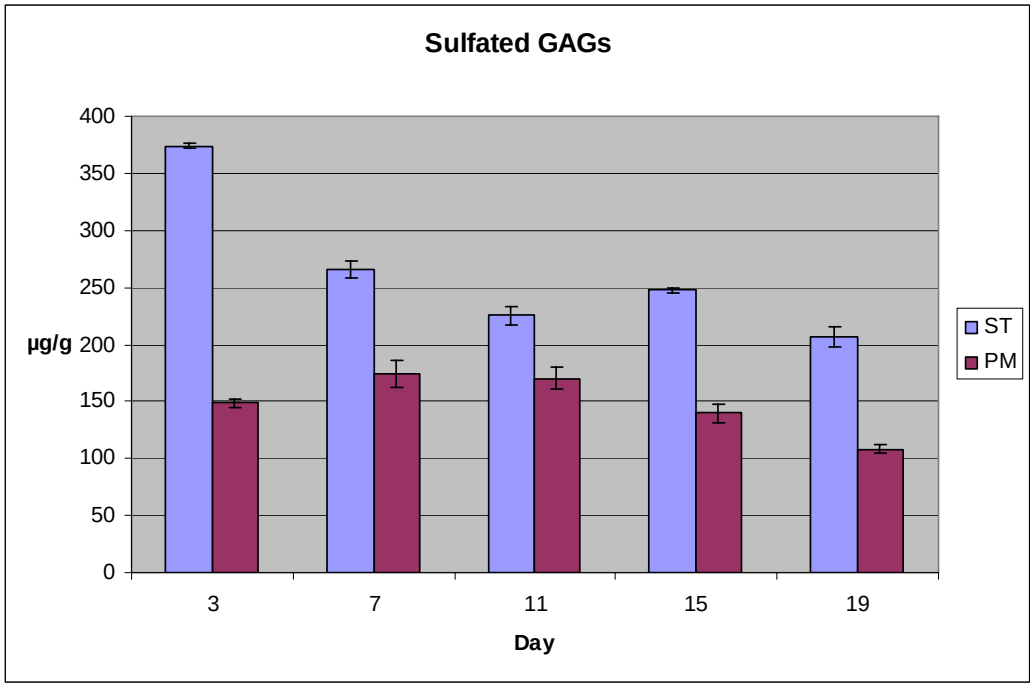

Figure 36: Shows the amount of sulfated GAGs in the muscles, M. semitendinosus (ST) and M. psoas major (PM) during the storage period. The values in ST was consistently higher than in PM.

The band at 1237 (Figure 37) has been discussed as referring to sulphate stretching vibration of proteoglycans (Camacho at al. 2001). This band shows an increase in absorption during storage for both muscles. 3 days post mortem storage has the lowest absorption in both muscles. In the ST muscle the difference between 3 and 7 days post mortem is the largest.

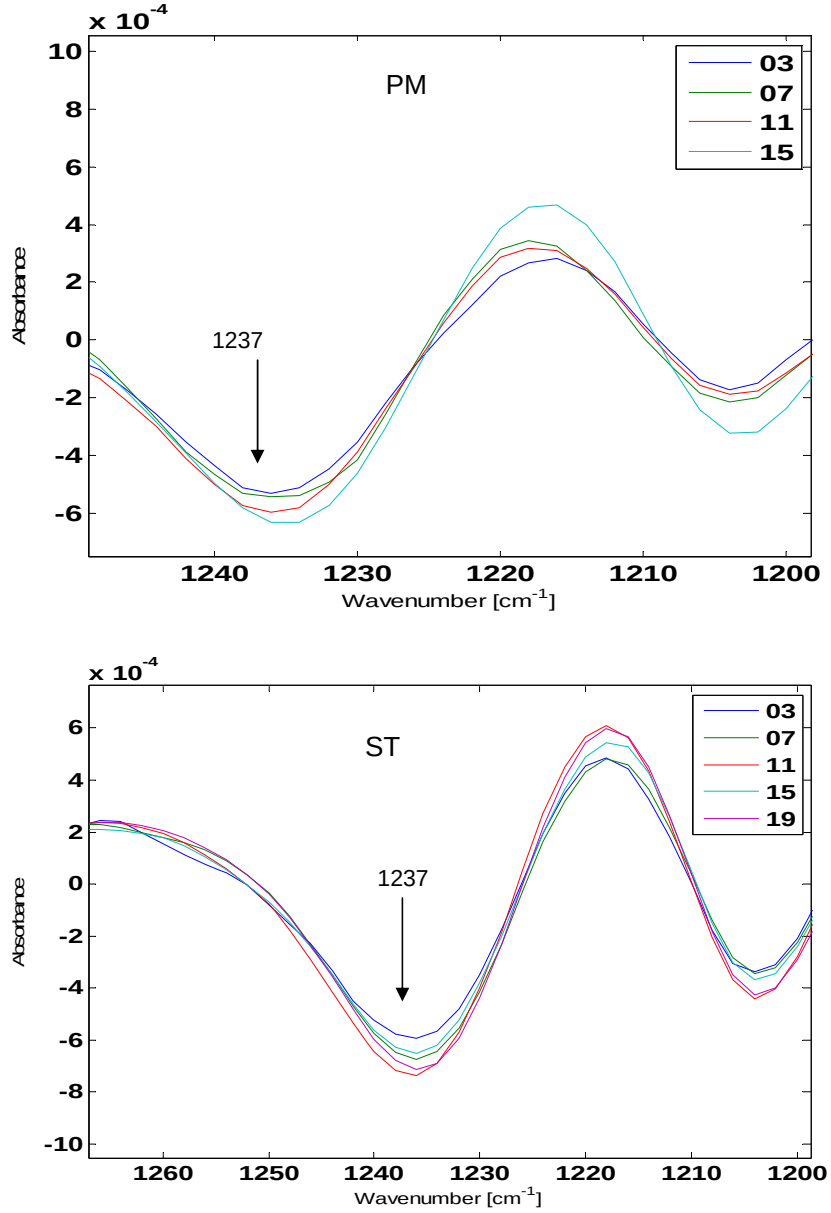

Figure 37: Shows the spectra from PM (left) and ST (right) at 1237 cm^{-1}.

The features at 1031, 1061 and 1082 cm^{-1} are assigned to C-O stretching vibration of the carbohydrate residues, which include both sulfated and non-sulfated GAGs. In both muscles there is a less obvious difference in the absorption due to storage. No clear tendency in degradation can be measured when measuring total GAGs. The non sulphated GAG represent hyaluronic acid (HA).

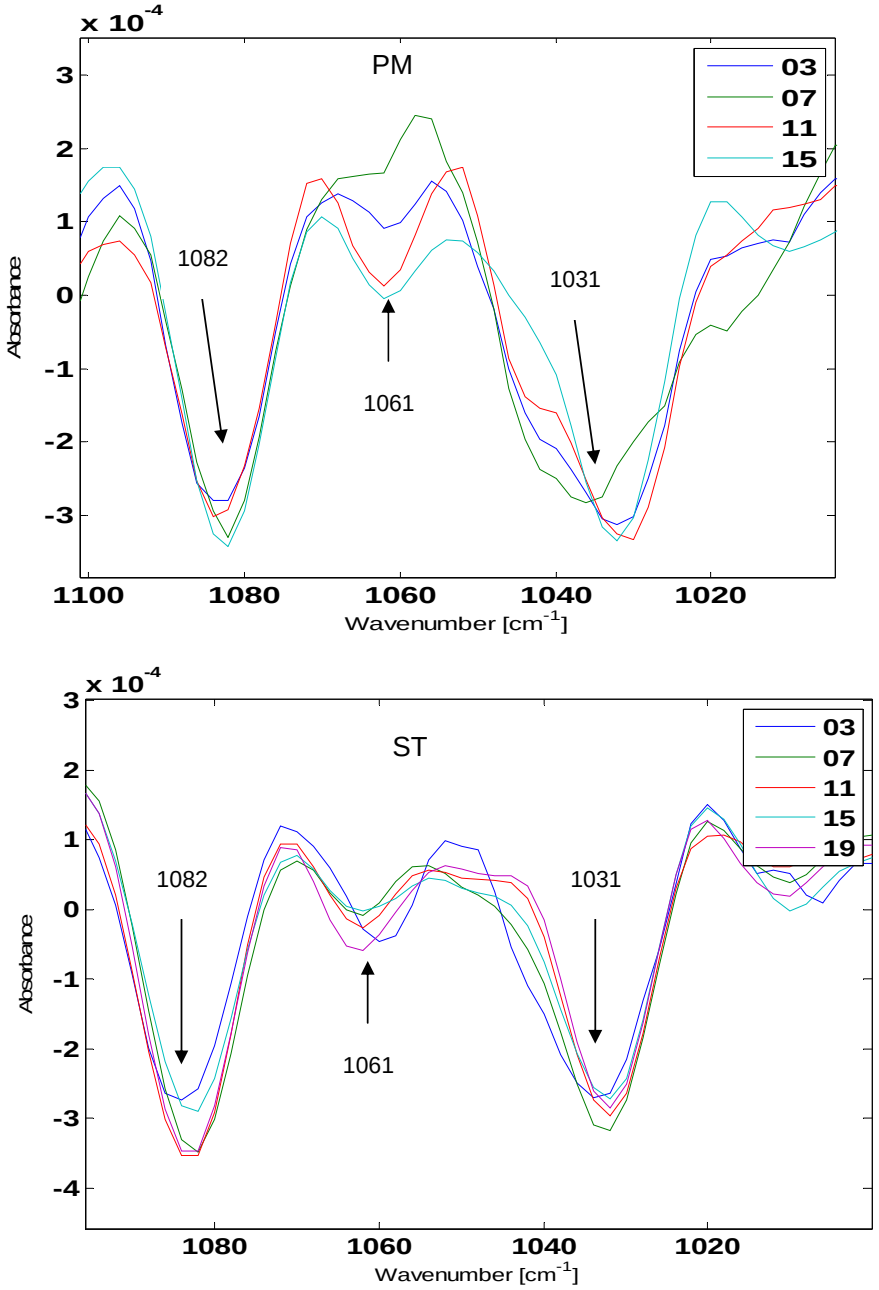

Figure 38: Shows the spectra from PM (left) and ST (right) between 1100 – 1000 cm^{-1}.

The amide A absorption around 3270-3310 cm^{-1}is give rise to N-H stretching which are hydrogen bonded. This can be due to water content in the sample. At ~3290 there is a

decrease in hydrogen bonding, and at ~3340 there is an increase in non-hydrogen bonded molecules. This can assume a reduction in water content during storage.

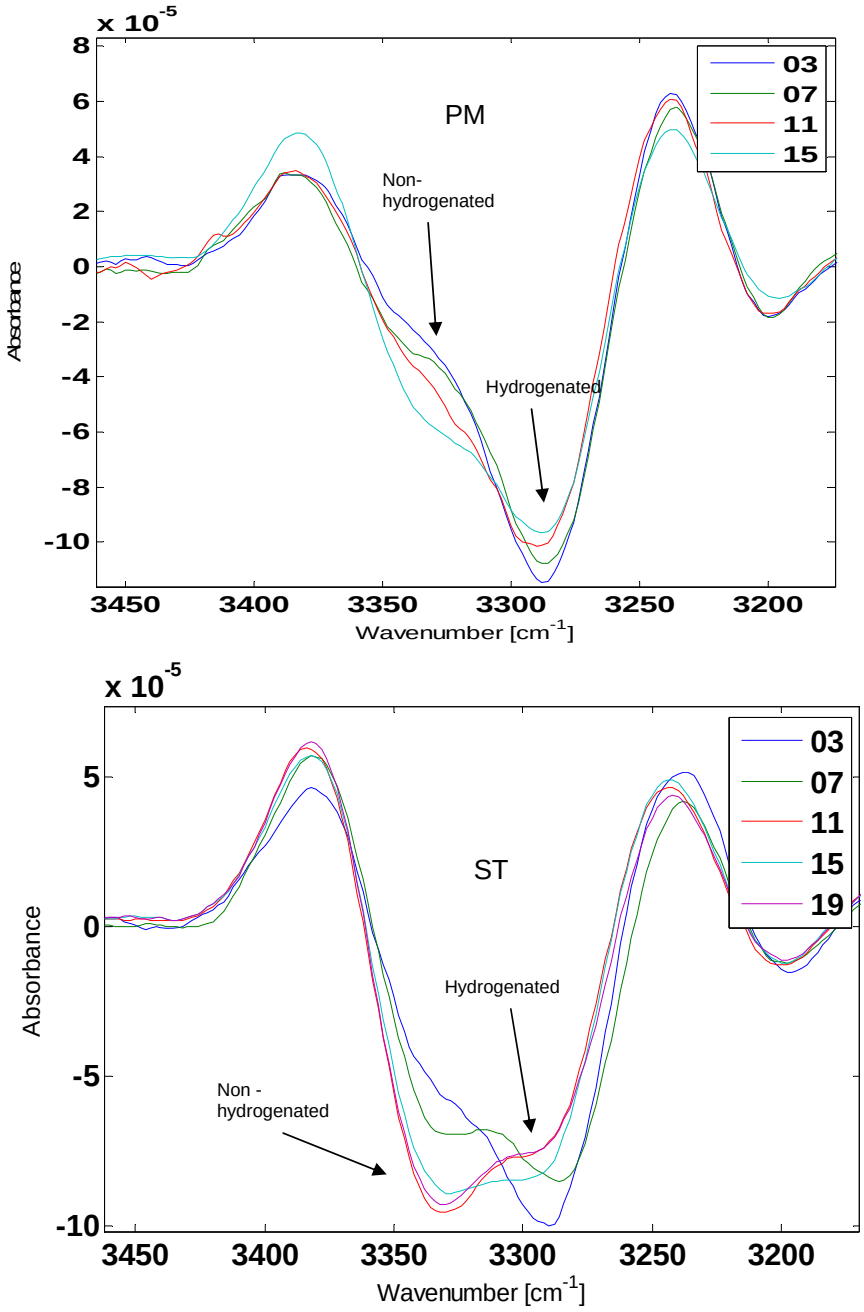

Figure 39: Shows the absorbance of hydrogenated and non- hydrogenated areas in the spectrum of PM and ST.

The spectra can indicate a difference in water content in the muscles. In figure 40 the spectra is plotted against the amounts of GAGs. GAGs attract water. The plot indicates a linear correlation due to decrease of water and decrease of GAGs during storage.

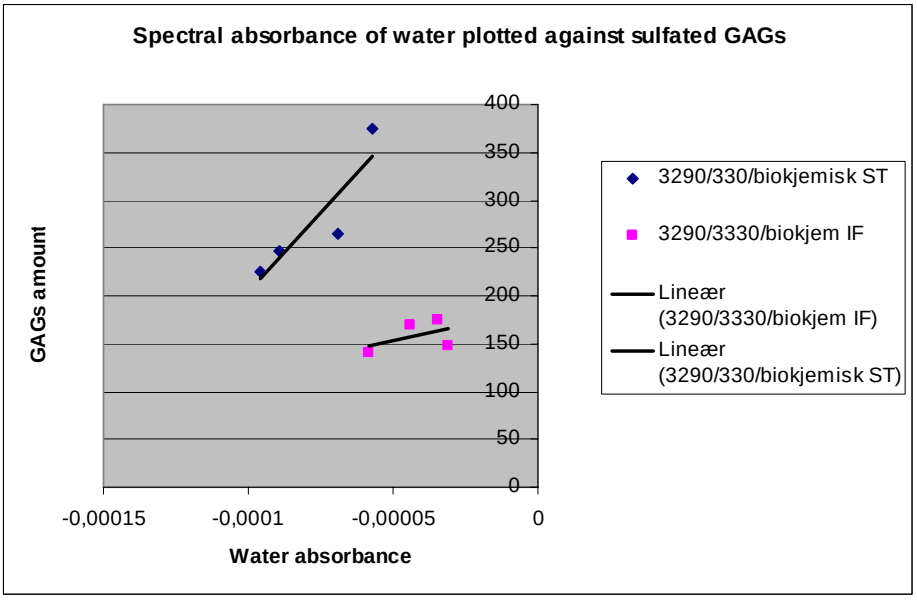

Figure 40: Spectral absorbance of water is plotted against the amount of sulfated GAGs at different storage time.

The PG content and distribution can be estimated in the samples by plotting PG/AmideI. This is done for the PM and the ST muscle. The image at 1240 shows how the collagen is distributed; higher absorbance corresponds to areas with high collagen content, which means that the red areas in the 1240 cm^{-1}contain most collagen. This is the area which will be analyzed. The red areas at the PG/Am I ratio image shows the ratio value due to the PG/collagen content.

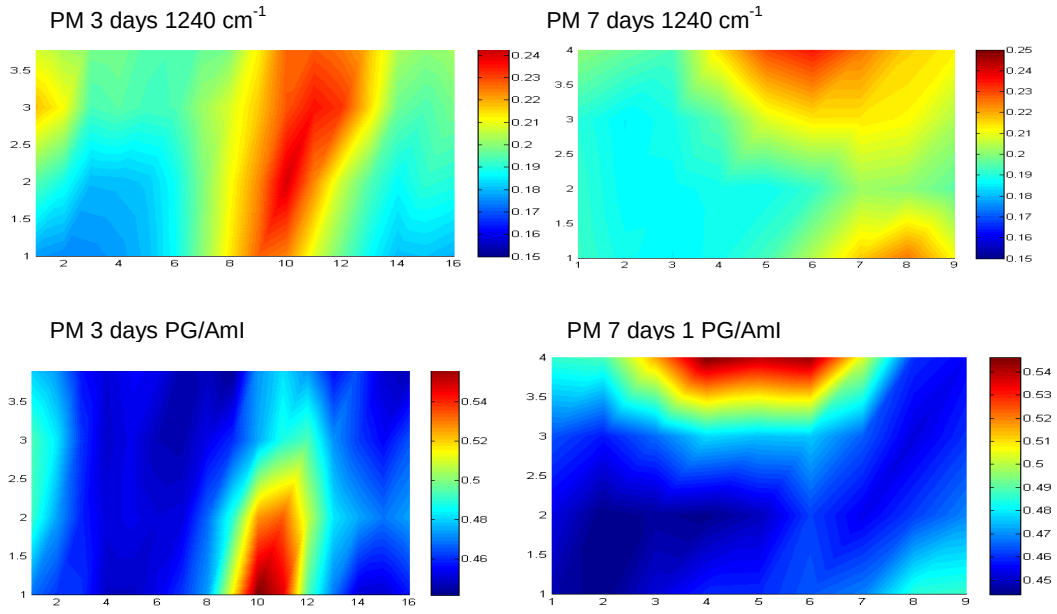

Figure 41: the image on the top shows the distribution of collagen in the PM muscle at 3 and 7 days post mortem. The image in the bottom shows the distribution of PG obtained from the PG/Amide I ratio.

The absorbance in the red area in the ratio PG/collagen images is similar at 3 and 7 days post mortem storage with value at approximately 0.54. The ratio values are quite high; this is due to the relative content of PGs and the amount/structure of collagen fibers present in the muscle. In the PM muscle the collagen fibers are more "loose" packed, so it could be more PGs in this network, compared to the network in ST muscle, where the collagen fibers is boned more closely together and there is less space for the PGs.
One can assume that the content of proteoglycans doesn't change during storage in the PM muscle.

The figure 41 shows the collagen content and distribution in the ST muscle at 3 and 11 days and the ratio PG/amide I. The red area in the 1240 cm^{-1} image is the area with most collagen. The blue/green area in the PG/AmI ratio image shows the ratio value due to the PG/collagen content.

The ratio value between PG/amide I seem to have a small increase during storage in the ST muscle. The ratio value is increasing from 0.11 to 0.14. The increasing in this value can indicate a structural change in the muscle during storage. The ST muscle has lower ratio

values, which indicates that the relative content of PGs is lower in this muscle compare to the PM muscle.

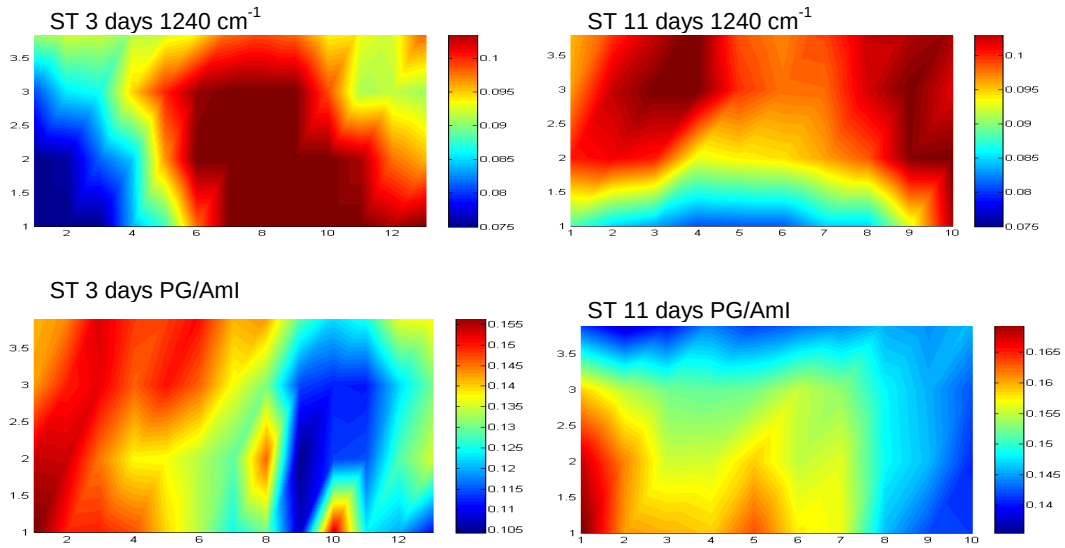

Figure 42: the image on the top shows the distribution of collagen in the ST muscle at 3 and 11 days post mortem. The image in the bottom shows the distribution of PG obtained from the PG/Amide I ratio.

Tissue section of ST and PM muscle were stained with Alcian Blue with 0.4M MgCl2, which is specific for detection of sulphated GAGs (Scott and Dorling, 1965). The intensity of the staining indicates the amount of sulfated GAGs in the connective tissue. Darker blue connective tissue contains more sulfated GAGs than lighter blue. The perimysium can be clearly seen as the main connective tissue in the microscope image. The figure 42 shows the microscopic image of the PM muscle after 3 and 7 days storage. There is a more intense staining at 3 days compared to 7 days post mortem storage. This can indicate that the amounts of GAGs are reducing during post-mortem storage. (The staining of the 7 days post mortem sample had an artefact, since the fibres got so blue).

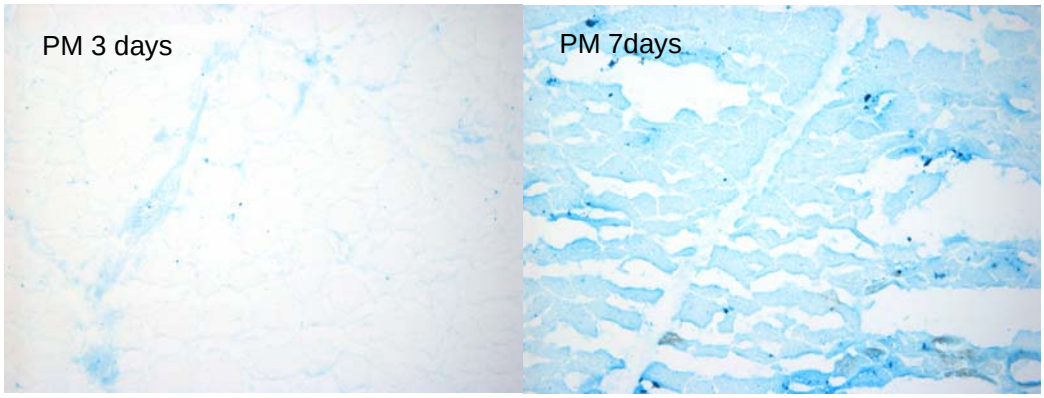

Figure 43: cross section of the PM muscle after 3 and 7 days, stained with Alcian blue,

The same staining pattern due to storage was also obtained for ST muscle (Figure 43). The more intense staining at 3 days post mortem shows that there is more sulphated GAGs present in the connective tissue of ST 3 days post mortem than 11 days post mortem.

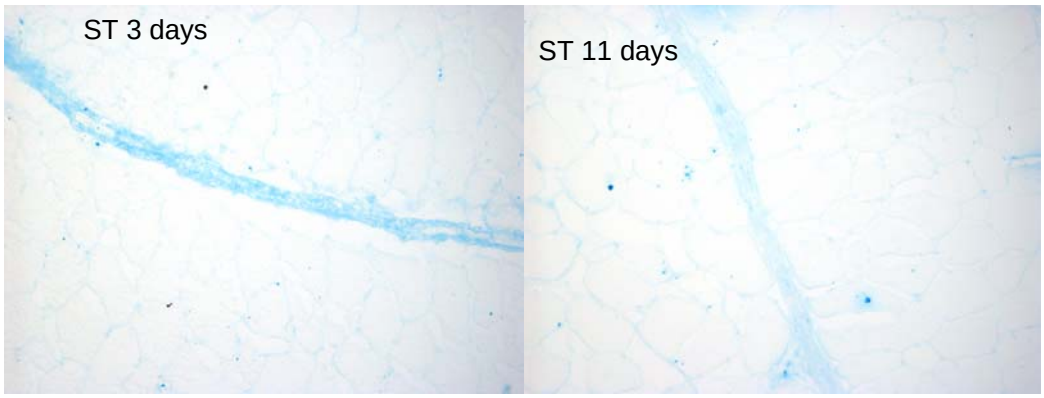

Figure 44: cross section of the ST muscle after 3 and 11 days, stained with Alcian blue. The blue colour is decreasing during storage which shows that the content of sulphated GAGs is degraded.

Comparing the different muscles, the connective tissue of ST muscle has a more intense colour than the PM, and thicker perimysium. Histology finding therefore supports the biochemical findings with more sulphated GAGs in the ST muscle compare to the PM muscle.

5. Discussion

In this study FTIR spectroscopy was related to biological components (parameters) of connective tissue that has been studied in relation to tenderness. Two models were used, skeletal muscles differing in texture properties and with different connective tissue composition, and post mortem storage, a process that has been in order to tenderize meat, and where these parameters is changed during the process. Biological parameters that has been evaluated due to tenderness has been collagen content (Bailey and Light, 1989, Pedersen *et al.* 1999), collagen cross-links (Bailey and Light, 1989), GAGs (Eggen *et al*, 1998) and structural organization of connective tissue (Eggen *et al*. 2001). Warner-Bratzler (WB) shear force was used as reference. A higher WB shear force value of ST reflected ST muscle to be tougher to PM. Both muscles also demonstrated tenderization due to storage, with a decrease in WB-value, and where ST muscle were consistently higher than PM until 15 days post mortem storage. Previous study has demonstrated higher shear force value of ST compared to PM immediately after slaughter (post motem 1 day). In this study, due to practical consideration at slaughter house, samples were collected at post mortem 3 days. One should therefore keep in mind that proteolytical processing and degradation of connective tissue components already have started, and the biological differences and structure is not that intact. Pedersen *et al* (2001) have demonstrated early post mortem degradation of proteoglycans complex already 48 h post mortem.

However, care should be taken to interpret directly the WB directly to textural properties of connective tissue. This as studies have demonstrated that it is difficult with regard to the contribution of connective tissue and myofiber (Møller, 1980).

FT-IR micro spectroscopy

The investigation of spatial variation in FT-IR micro spectroscopy is a very important issue. In the spectra some information can be hidden under big absorbed bands. To resolve nearby lying bands the spectra were derivatised (second derivative) using the algorithm by Savitzky-Golay. Then the spectra were then pre-processed by physical extended multiplicative signal correction (EMSC) to remove baseline shifts, multiplicative and wavenumber-dependent scatter effects.

Spectroscopy and collagen parameters

The major feature in the spectra is the amide I absorption band between 1610-1690 cm^{-1}. This spectral region is difficult to analyse and great care should be taken in any interpretation of spectral differences between tissues (Jackson *et al*. 1995).
The band at 1659 arises from possible non- reducible collagen cross-links (Miller *et al*. 2004, Paschalis *et al.* 2001, Paschalis *et al.* 2003 and Camacho *et al*,. 2001). The PM muscle shows a decrease in absorbance during storage, this can be considered to indicate a reduce in the amount of non-reducible cross-links. In the ST muscle the spectra is more random. This can indicate that there are more cross-links in the ST muscle and the fibers can be more tightly bonded. More tightly bound collagen would be less vournable to degradation by proteolytic enzymes. The staining of collagen I showed that the distribution of the epitopes recognized by the antibody differed between the two muscles. However, collagen I staining by antibodies is a non-quantitative method, and therefore a reduction in collagen amount or crosslinks due to degradation can not be verified by this method. Quantification of crosslinks by HPLC should be performed to verify this difference in FTIR spectra observed. Picorius red is a more quantitative method of collagen staining; unfortunately we could not use this method due to HMS rules at Nofima Mat AS. However, the staining with collagen I antibodies shows that there are differences between the two muscles. The perimysium of ST muscle showed a wavy appearance with clear thread-like like structures, in contrast to PM which showed a more diffuse staining pattern of the perimysium. This could support some difference in collagen organization between the two muscles, which could affect the collagen degradation in the two muscles. This is also shown earlier by electron microscopy, where the ST muscle tend to have a more tightly bounded collagen fibers than PM (Eggen *et al.,* 2001), supporting collagen bundles less vournable to proteolytic attack. If the collagen had been more degraded one could expect more disintegrated areas by collagen I staining. The immonostaing also show that there is a huge intramuscular variation due to collagen staining. It is therefore difficult to interprent difference in degradation between the two muscles and post mortem.

Our FTIR results indicate some structural changes of collagen due to post mortem storage. The change was more obvious in PM muscle. This could again support a different organization of collagen in PM and ST muscle as mentioned above, with less tightly bounded collagen fibers in PM muscle, being more accessible to structural changes post mortem. The band at 1654 cm^{-1} represents the α-helix in the collagen molecule (Jackson and Mantsch.

1995). The PM muscle shows a decrease in the absorbance during aging time, which can indicate a structural change in the connective tissue. The electron density in the C=O group is getting lower; one can assume that the α-helix-complex decomposed.

The band at 1340 cm^{-1} is discussed to be a marker for collagen (Camacho *et al* 2001, and Jackson *et al* 1995). At this absorbance both of the muscles tend to make two groups. The spectra from 3 and 7 days post mortem of are grouped together and the spectra from 11, 15 and 19 days seem to be grouped. The 11, 15 and 19 group shows a higher absorbance than the 3 and 7 days post mortem storage group. This can indicate a structural changing of collagen. Our FTIR data indicated loss of water due to post mortem storage (the 3290 peak). One can assume that the decreasing of water content may make the collagen more accessible for absorbance and that the relative amount is getting higher. Nishimura, T. (2010) has showed that during post mortem the linkage between collagen fibrils is weakened.

Another band which can indicate the amount of collage is at 1282 cm^{-1}. This is attributed to the amide III, a complex vibrational band having components due to C-N stretching and N-H in plane bending from amide linkages. The absorptions band 1282 is suggested to come from the glycine backbone and proline side chains (Jackson *et al.,* 1995). In the PM muscle the 15 days post mortem absorption is much higher than 3,7 and 11 days post mortem storage absorbance. In the ST muscle there is a clear grouping from the spectra from 3 and 7 days post mortem to the 11,15 and 19 days post mortem. One can consider that the structural changing is faster in PM, because of the bigger difference between 15 days post mortem to the other.

The orientation of collagen fibrils is obtained from polarization measurement. The transition moment of the amide I vibration of collagen, which means essentially, the direction of the bond vibration, is approximately perpendicular to the collagen long axis. The transition moment of the amide II vibration of collagen is parallel to the long axis. The sample are analyzed at a polarization angle at 0 º and 90 º, and then the ratio between amide I at 0º and amide I at 90º is calculate. This ratio indicates the direction of the collagen fiber. The PM muscle had a ratio at approximately 1 which corresponds to none orientation. All the fibers seem to be random orientated. In our immonohistological staining with collagen I of the PM muscle, the collagen fibers in the perimysium doesn't show any clear structure. In comparison with the stained ST muscle, some of the collagen fibers and their direction can be seen in the

perimysium. The electron microscopy image (Eggen *et al,* 2001) shows that the collagen fibrils in ST are more organized. The ratio between amide I at 0º and amide I at 90º indicate that the collagen fibers are more oriented at day 3 post mortem than in day 11 post mortem. It is assumed that there is a structural change during storage, and that the collagen fibril is degraded.

Spectroscopy and GAG parameters

The amount of sulfated GAGs where analyzed both biochemical, histological and with spectroscopic methods in this experiment. GAGs consist of repeating disaccharide modified by sulfate, and where the carboxylate and sulfate groups give the molecules strong anionic properties with water binding properties. Both sulfate and carbohydrate residues have spectral absorption.
The biochemical results show a total decrease in sulfated GAGs content in both muscles. The sulfated GAG content in ST was consistently higher than PM during the whole storing period. This can also be supported by the Alcian blue staining of cryo-section of the two muscles. The Alcian blue staining indicates the amount of sulfated GAGs in the connective tissue, and outline a thicker perimysium of ST compared to PM, reflecting more amount of connective tissue and therefore sulfated GAGs. The staining intensity was stronger at 3 days post mortem than 7 and 11 days post mortem storage for both muscles. FTIR analysis support the biochemical and histological finding. In the FT-IR spectra there is a difference in the sulfate stretch absorbance during storage post mortem. The absorbance at 1237 cm^{-1} refers to sulfate stretch in proteoglycans. The 3 and 7 days post mortem storage are grouped together from the 11, 15 and 19 days post mortem storage in both muscles. The largest difference measured biochemically is due to 3 and 7 days post mortem storage of ST muscle, this can also be seen in the spectra.

In the spectra measuring carbohydrate residues (1031, 1061 and 1082 cm^{-1}), there is however no clear tendency in differences between the two muscles. The carbohydrate residues represent both sulfated and non sulfated GAGs (HA). In a previous study by Pedersen *et al*

(1999), no difference in total amount of GAGs quantified by measuring hexuronic acid was observed in ST and PM muscle, supporting this FTIR finding.

The intensity of 1237 cm^{-1} band is increasing during storage in both muscles. Compared to the biochemical analysis this indicates the opposite result. The GAGs are linear structures linked to a protein core; a conformation change would have resulted in a shift in the spectra, which we don't have.

The increasing of the absorbance can be due to the water content and a different structural organization. Degradation of the PGs may be caused by several enzymes and aggrecanases, this probably involves both degradation of the GAGs as well as the peptide core (Hannseson *et a.* 2003, Nishimura *et al*. 1996). With this breakdown the structures will collapse, but the sulfate group and COO^- will still be attached to the molecule, and the molecule may be more accessible for infrared absorption.

The amide A absorbance shows the N-H stretching and hydrogen bonding. The frequency is dependent on the strength of the hydrogen bond. Hydrogen (H^+) is positively charged and nitrogen is negatively charged. There is a dipole, and the hydrogen bond will weaken the dipole linkages which give a lower absorbance number (Barth, A., 2007). The hydrogenated bond have an decrease in the absorbance while the non-hydrogenated bond increases. This gives more N-H without hydrogen bond during storage. This will give the sulfate groups more space and more accessible for infrared absorption. Plotting the water absorbance against the amount of GAGs support the decrease of water content. GAGs attracts water, the degradation of GAGs will reduce the amount of water.

Eggen et al. (1998) has shown that PGs and GAGs degrade during storage. Molecules that contain chondrotin/dermatan sulfate with both high and low molecular mass have been identified in adult bovine M. *semimembranosits* (Eggen et al. 1994). It is not possible to suggest the contribution of the separate proteoglycans families to the reduced content of GAGs in the extract and the sulfate stretch 1237 cm^{-1}. The different proteoglycans may be involved in the degradation at different times. The small proteoglycan decorin is showed to be degraded during post mortem (Hanneson, K et al 2003).The degradation of decorin involves both the carbohydrate chain and the protein core. The anionic charge of the decorin molecule is provided by sulfate and carboxyl groups in the carbohydrate side chains. The reduction in the amount of anionic material and negatively charged ions needed to elute the molecules observed in ion exchange chromatography, is most likely a result of loss of these groups in the

molecules (Eggen et al., 1998).The muscle tissue contains hyaluronate (Laurent and Fraser, 1992) which can form large aggregates with aggrecan-like proteoglycans. Aggrecan is a strong water binder and it has been together with HA demonstrated to be degraded early post mortem (Hannesson, K. *et al*., 2003). The degradation observed may be a result of breakdown of the aggregates as well as the large aggrecan-like proteoglycans. Aggrecan are also highly sulfated, and contain many GAGs, compare to decorin which only have one GAG chains attached. On can assume that the aggrecan decomposition contribution in FT-IR spectra are most likely best detected, also since the water content is decreasing.

Due to the polarization images, the monitoring of PG is based on molecular vibration in the sugar region (PG area). The ratio between the PG sugar absorbance to amide I has previously been correlated to specific quantities of aggrecan and collagen mixtures in a series of model compounds (Camacho *et al.,* 2001). The ST muscle obtained a small increase in PG/collagen ratio value from 3 to 11 days post mortem storage. The PM muscles showed similar values at both storing times . The PGs may be degraded faster in the ST muscle compared to the PM muscle. The PM muscle shows a higher absorbance than the ST muscle in the polarization images. This could reflect more degradation of GAG/collagen ratio of ST compared to PM. This can be due to the differences in structural organisation in the two muscles. Previous studies by Eggen *et al*. 1998 have confirmed a higher GAG/collagen ratio in PM muscle than ST muscle, confirming our FTIR data of PG sugar absorbance to amide I.

6 Conclusions

This work shows some correlation between FTIR spectra and biological parameters.
The results showed that aging time had an effect on the spectra at different wavelengths. The collagen absorption showed a tendency to decomposition of the α-helix and some indication about degradation of cross-links in the PM muscle. The collagen fibers in the PM muscle showed to have a more random orientation, than the fibers in the ST muscle which showed an orientation parallel to the x- axis early in the period, and a more random orientation after 11 days post mortem storage. This is supported by the collagen I staining, where the perimysium of PM which showed a more diffuse staining pattern compared to the ST muscle which shows a more wavy appearance with clear thread-like like structures.
The ST muscle had consistently higher content of sulfated GAGs than the PM muscle due to the biochemically and histological analysis. The FT-IR spectra showed the same tendency. The content of sulfated GAGs showed a decrease in both muscles during storage. It is well known that the GAGs attracts water, and the degradation of GAGs could reflect the decrease in water absorbance obtained in the spectra, further supporting a good correlation between FI-IR and biological componets.

FT-IR micro spectroscopy is promising in evaluating connective tissue in bovine skeletal muscles. Further studies with more animals are needed to statistically verify the use of spectroscopic methods to measure biological components. It would also be interesting to investigate further the possibility of measure each GAG type by FT-IR micro spectroscopy. This study showed that FT-IR can be used on different types of tissue, besides cartilage and bone, as shown in earlier studies.

7 References

Avery, N.C., Sims, T.J., Warkup, C. and Bailey, A. (1996) Collagen cross-linking in porcine m. Longgissimus lumborum: absence of a relationship with variation in texture at pork weight. *Meat Science* 42, 355-369.

Bailey, A. and Light, N. (1989) Connective tissue in meat and meat products. Elsevier applied science, UK.

Bailey,A .J. 1972. The basis of meat texture. *J. Sci.Food Agric*. 23:995

Bailey, A..J., Restall, D.J,, Sims, T. and Duance V. (1979) Meat tenderness: Immunofluorescent localisation of the isomorphic forms of collagen in bovine muscles of varying texture. J.*Sci.Food Agri*. 1979, 30, 203-210.

Barth, A. (2007) Infrared spectroscopy of proteins. *Biochimica et Biophysica Acta 1767*, 1073-1101.

Bi, X., Li, G., Doty, S.B. and Camacho, N.P. (2005) A novel method for determination of collagen orientation in cartilage by Fourier transform infrared imaging spectroscopy (FT-IRIS) *OsteoArthritis and cartilage*, 13, 1050-1058.

Bi, X., Yang, X., Bostrom, M.P.G.and Camacho N.P.(2007) Fourier transform infrared imaging and MR microscopy studies detect compositional and structural changes in cartilage in a rabbit model of osteoarthritis. *Anal. Bioanal Chem*, 387:1601-1612

Bolis, S., Handley, C., and Comper W.D. (1989). Passive loss of proteoglycans from articular cartilage explants. *Biochim. Biophys. Acta*. 993, 157-167

Brooks, J.C. and Savell, J.W. (2004) Perimysium thickness as an indicator of beef tenderness. *Meat Science*, 67, 329-334.

Brown, M., West, L., Merritt, K. and Plaas, A. (1998) Changes in sulfation patterns of chondroitin sulfate in equine articular cartilage and synovial fluid in response to aging and osteoarthritis. *Am. J. Vet. Res*, 59, 786-791.

Bychkov, S.M. and Kuz`mina, S.A. (1992)Study of tissue proteoglycans by means of infrared spectroscopy. *Biull Eksp. Biol. Med*. 114(9), 246-249

Bychkov, S.M. and Kuz`mina, S.A. (1991)The comparative study of the IR spectra of proteoglycans. *Biull Eksp. Biol. Med*. 112(11), 480-482

Carey, D. Syndecans: multifunctional cell-surface co-receptors.*Biochem*.J.1997,327,1-16.

Camacho, N.P., West, P., Torzilli, P.A. and Mendelsohn, R. (2001) FTIR microscopic imaging of collagen and proteoglycan in bovine cartilage. *Biopolymers* 62:1-8.

Casu, B.; Petitou, M; Provasoli, M. and Sinay, P.(1988) Conformational flexibility: a new concept for explaining binding and biological properties of iduronic acid-containg glycosaminoglycans. *Trends Biochem.Sci*. 13,221-225.

Colthup, N.B., Daly, L.H. and Wiberley, S.E. (1975) Introduction to Infrared and Raman Spectroscopy, 2nd ed.Academic Press, New York, 1975.

Danielson, K.G, Baribault, H., Holmes, D.F., Graham, H., Kaldler, K.E. and Iozzo R.V (1997) Targeted disruption of decorin leads to abnormal collagen fibril morphology and skin fragility. J. Cell Biol 1997; 136:729-743.

DeNoyer, L.K. and Dodd, J.G. (2002) Smoothing and derivates in spectroscopy. In:*Handbook of Vibrational Spectroscopy*, vol 3 eds J.M. Chalmers and P.R. Griffiths,pp 2173-2183 Chichester. UK: John Wiley & Sons Ltd

Dutson, T.R and Lawrie, R.A. (1974)Release of lysosomal enzymes during post mortem conditioning and their relationship to tenderness. *J. Food Tecnol*., 9,43.

Eggen, K.H., Ekholdt, W., Høst, V. and Kolset, S. (1998) Proteoglycans and meat quality- a possible role of chondroitin/dermatan sulfate proteoglycans in post mortem degradation. *Basic. Appl. Myol.* 8, 159-168

Eggen, K.H., Malmstrøm, A. and Kolset, S. (1994) Decorin and a large dermatan sulfate proteoglycan in bovine striated muscle. *BBA* 1204, 287-297

Eggen, K.H., Malmstrøm, A., Sørensen, T. and Høst, V. (1997) Identification om proteoglycans in bovine M. semimembranosus by immunohistochemical methods. *Journal of muscle Foods*, 8, 121-136.

Eggen, K.H. and Buer, W. (1991) Post mortem changes of glycoconjugates in meat. *Proceeding at 37 th International Congress in Meat Science anf Technology*, 1, 344-347

Eggen, K.H., Pedersen, M.E., Lea, P. and Kolset, S. (2001) A comperativ study on the structure and solubility om collagen and glycosaminoglycans in two bovine muscle with different textural properties using transmission electron microscopy and biochemical methods. *Journal of Muscle Foods*, 12; 245-261.

Esko, J.D., Kimata, K. and Lindahl, U. (2009) Proteoglycans and Sulfated Glycosaminoglycans I: Varki A, Cummings RD, Esko JD *Essentials of Glycobiology*. 2nd edition. Cold Spring Harbor (NY); USA

Fransson, L.Å and Cøster, L.(1979) Interaction between dermatan sulphate chains. I Affinity chromatography of copolymeric galactosaminoglycans on dermatan sulfate-substituted agarose. *Biochem.Biophys. Acta*, 582, 132-144.

Halberg, D.; Proulx, G.; Doeges, K.; Yamada, Y.;Drickamer, K. (1988)A segment of cartilage proteoglycan core protein has lecitin-like activity. *J. Biol. Chem*.,263, 9486-9490

Hannesson, K., Pedersen, M.E., Ofstad, R., Kolset, S.O. (2003). Breakdown of large proteoglycans in bovine intramuscular connective tissue early post mortem. *Journal of Muscle Foods,* Vol 14, 265-351.

Harper, G.S. (1999) Trends in skeletal muscle biology and the understanding of toughness in beef. *Aust. J. Agri. Res*. 50, 1105-1129.

Iozzo, R.V. (1994). "Perlecan: a gem of a proteoglycan". *Matrix Biol.* **14** (3): 203–8
Ippolito, E.; Pedrini, V.A. and Pedrini-Mille, A. Histochemical properties of cartilage proteoglycans. *J. Histochem. Cytochem*. 31(1) 53-61 (1983).

Iozzo, R.V. (1998) Matrix proteoglycans: From Molecular Design to Cellular Function. *Annu. Rev.Biochem*, 67, 602-652.

Ippolito E, Pedrini VA, Pedrini-Mille A (1983) Histochemical properties of cartilage proteoglycans. *J Histochem Cytochem* 31:53–61

Jacksen, M., Choo, L-P., Watson P.H., Halliday, W.C., and Mantsch, H.H. Beware of connective tissue proteins: assignment and implications of collagen absorptions in infrared spectra of human tissues. (1995) *Biochim Biophys Acta* 1270:1-6

Jacksen, M and Mantsch, H.H. (1995) The Use and Misuse of FTIR Spectroscopy in the Determination of Protein Structure. *Biochemistry and Molecular Biology,* 30(2):95-120 (1995).

Jalkanen M, Elenius K, Inki P, Kirjavainen J, Leppa, S(1991) Syndecan, a regulator of cell behaviour, is lost in malignant transformation. *Biochem. Society trans*. 19, 1069-1072.

Jepsen K.J., Wu, F., Peragallo, J.H., Paul, J., Roberts, L., Ezura, Y., Oldeberg, A., Birk. D.E. and Chakravarti, S. (2002) A syndrome of joint laxity and impaired joint integrity in lumican- and fibromodulin- deficient mice. *J. Biol. Chem*, 277:35532-35540

Judge, M., Aberle, A., Forrest, J., Hedrick, H. and Merkel, R. (1989) Principles of meat science (2nd edition). Kendall/Hunt publishing company.

Junquiera L, C.U, Bignolas G, Brentani RR (1979) Picrosirius staining plus polarization microscopy, a specific method for collagen detection in tissue sections. Histochem J 11:447-455

Kadler, K.E., Holmes, D.F., Trotter, J.A. and Chapman, J.A (1996) Collagen fibril formation. *Biochem* 316:1-11

Kim M, Bi X, Horton WE, Spencer RG, Camacho NP (2005) Fourier transform infrared imaging spectroscopic analysis of tissue engineered cartilage: histologic and biochemical correlations. J *Biomed Opt*. 2005:10(3):031105.

Formatert: Skrift: Fet
Formatert: Skrift: Times New Roman, Fet
Slettet: c
Formatert: Skrift: Times New Roman, Fet
Slettet: u
Formatert: Skrift: Times New Roman, Fet
Formatert: Skrift: Times New Roman

Kirschner, C, Ofstad, R, Skarpeid, H.-J., Høst, V and Kohler K (2004) Monitoring of Denaturation Processes in Aged Beef Loin by Fourier Transform Infrared Microspectroscopy. *J. Agric. Food Chem.*, 2004, *52* (12), pp 3920–3929

Kohler,A., Bertrand, D., Martens,H., Hannesson, K., Kirschner, C. and Ofstad, R. (2007) Multivariate image analysis of a set of FTIR microspectroscopy images of aged bovine muscle tissue combining image and design information. Volume 389, Number 4, 1143-1153, DOI: 10.1007/s00216-007-1414-9.

Kohler, A.; Kirschner, C.; Oust, A.; Martens, H (2005). Extended Multiplicative Signal Correction as a Tool for Separation and Characterization of Physical and Chemical Information in Fourier Transform Infrared Microscopy Images of Cryo-sections of Beef Loin. Volume 59, Issue 6, Pages, pp. 707-716(10).

Krimm and Bandekar, (1986) Vibrational spectroscopy
and conformation of peptides, polypeptides and proteins. Protein Chem.. 38.181-364.

Laurent, T.C and Fraser, J.R.E. (1992) Hyaluronan. *FASEB J*. 6, 2397-2404.

Lazarev, Y.A. and Lazarev, A.V. (1978). Infrared spectra and structure of synthetic polytripeptides. *Biopolymers* 17:1197-1214

Lazarev, Y.A., Grishkovsky, B.A. and Khromova, T.B. (1985) Amide I band spectrum and structure of collagen and related polypeptides. *Biopolymers* 24:1449-1478.

Lewis, G.J., Purslow P.P., and Rice. A.E. (1991) The effect of conditioning on the strength of perimysial connective tissue dissected from cooked meat. *Meat science*. 30, 1-12.

Light, N.D., Champion, A.E., Voyle, C. and Bailey, A.J. (1985) The rôle of epimysial, perimysial and endomysial collagen in determining texture in six bovine muscles. *Meat Science*, 13, 137-149.

Locker, R.H., and Hagyarda, C.J. (1987)A cold shortening effect in beef muscle Light, N. D. In: Advances in meat research, vol 4, ed. A.M Pearson, T.R. Dutson & A.J. Bailey. Van Nostrand Reinhold, New York.

Maroudas, A., Muir, H. and Wingham, J. (1969). The correlation of fixed negative charge with glycosaminoglycan content of human articular cartilage. *Biochim. Biophys. Acta*. 117, 492-500

Martens,H., Nielsen, J.P. and Engelsen, S.P. (2003) Light Scattering and Light Absorbance Separated by Extended Multiplicative Signal Correction. Application to Near-Infrared Transmission Analysis of Powder Mixtures. *Anal. Chem.*, 2003, *75* (3), pp 394–404

McMurry, J. (2004). Organic Chemistry. London, UK:Brooks/Cole.

Miller, L.M., Novatt, JT Hamerman, D. Carlson CS. (2004) Alterations in mineral composition observed in osteoarthritic joints of cynomolgus monkeys. *Bone*. 35:498-506.

Murphy, G., Coekett, M.I., Ward, R.V. and Docherty, A.J.P. (1991) Matrix metalloproteinase degradation of elastin type IV collagen and proteoglycans. *Biochem. J*. 277, 277-279

Møller, A. (1980) Analysis of Warner Bratzler shear pattern with regard to myofibrillar and connective tissue components of tenderness. *Meat Sci*. 5, 247-260

Møller, P.W., Field, P.A., Dutson, T.R., Landmann, W.A. and Carpenter, Z.L. (1976) Effect of high temperature conditioning on subcellular distribution and levels of lysosomal enzymes.. *J. Food Sci*., 41. 216-217.

Nishimura, T. (2010).The role of intramuscular connectic tissue in meat texture. Animal Science Journal 81, 21-27.

Nishimura, T., Hattori, A. and Takahashi, K. (1996) Relationship between degradation of proteoglycans and weakening of the intramuscular connective tissue during post-mortem aging of beef. *Meat Science* 42, 251-260

Nishiumi, T.; Kunisshima, R.; Nishimura, T. and Yoshida, S. (1995) Intramuscular connective tissue components contributing to raw meat thoughness in various porcine muscles. *Animal Science Journal 66,* 341-348.

Owen, A.J. (1995) Uses of Derivate Spectroscopy. Agilent Technologies, Publication nr 5963-3940E

Offer , G. and Knight, P. (1988). The structural basis of water-holding in meat. Part1:General principle and water uptake in meat processing. In *Developments in Meat Science*, vol 4 (ed Lawrie), pp63-172. Barking, Essex: Elsevier Science Publishers Ldt.

Paschalis, EP., Ilg, A., Verdelis, K., Yamauchi, M., Mendelsohn, R. and Boskey A.L. (1998). Spectroscopic determination om collagen cross-links at the ultrastructural level and its application to osteoporosis. *Bone* 23:S342

Paschalis, EP., Verdelis, K.,Doty SB., Boskey, AL., Mendelsohn, R. and Yamauchi, M. (2001)Spectroscopic Characterization of Collagen Cross-Links in Bone *J Bone Miner Res* 16:1821-1828.

Paschalis, EP., Recker, R., DiCarlo, E., Doty S.B., Atti, E. and Boskey, A.L. (2003) Distribution of Collagen Cross-Links in Normal Human Trabecular Bone. *J Bone Miner Res* 18:1942-1946.

Pavia, D.L., Lampman, G. M. and Kriz, G. S. (2001) Introduction to spectroscopy, 3rd edition, Wahington, USA: Thomson Learning

Pedersen, M.E., Kolset, S., Sørensen, T. and Eggen, K.H (1999) Sulfated Glycosaminoglycans and Collagen in Two Bovine Muscles (M. *semitendinosus* and M. *psoas major*) Differing in Texture. *J. Agric. Food. Chem*. 47, 1445-1452.

Pedersen, M.E., Kulseth, M., Kolset, S., Velleman, S. and Eggen, K.H. (2001) Decorin and fibromodulin expression in two bovine muscles (M. *semitendinosus* and M. *psoas major*) differing in texture. *J. Muscle Foods*, 12/1, 1-17

Purslow, P. (2002)The structure and functional significance of variations in the connective tissue within muscle. *Comparative Biochemistry and Physiology Part A: Molecular & Integrative Physiology*,133, 947-9666.

Purslow, P.P. and Trotter, J.A (1994). The morphology and mechanical properties of endomysium in series-fibred muscle; variation with muscle length. *Journal of Muscle Research and Cell Motility*, 15, 299-304

Recklies, A.D, Poole, A.R., Banerjee, S. et al. (2000) Pathophysiologic aspect of inflammation in diarthrodial joints. In: Buckwalter, J.A. Einhorn, T.A. Simon, S.R. eds. Orthopaedic Basic Science: Biology and biomechanics of the Musculoskeletal System, 2nd ed. Rosemont, IL;American Academy of Orthopaedic Surgeons, 489-530.

Reiser, J.M., McCormick, R.J. and Rucker, R.B. (1992). The enzymatic and non-enzymatic crosslinking of collagen and elastin. FASEB J. 6:2439-2449

Rowe, R.W.D. (1981) Morphology of perimysial and endomysial connective tissue i skeletal muscle. *Tissue Cell*, 13, 681-690

Savitzky, A. and Golay, M. J. E (1964) Smoothing and Differentiation of Data by Simplified Least Squares Procedures. *Anal. Chem.*, 1964, *36* (8), pp 1627–1639

Scott, J.E.;Heatley, F and Wood, B. (1995) Comparison of secondary structures in water of chondrotin-4-sulfate and dermatan sulphate: Implication in the formation of tertiary structures. *Biochem*. 34,15467-15474.

Sink, J., Turgut, H., Mann, O., Weakley, D. and Escoubas, J. (1983) Effect of age and sex on the biophysical properties of fresh beef muscle from bullocks and steers. *J. Food Sci*., 48, 844-847.

Socrates, G. (2001) Infrared and Raman Characteristic Group Frequencies, third edition. London, UK, John Wiley & Sons, LTD

Stanton, C. and Light, N. (1987). The effects of conditioning on meat collagen: Part 1—Evidence for gross *in situ* proteolysis. Meat science 21, 249-265.

Stuart, B. (1197) Biological application of infrared spectroscopy. Chichester, UK: John Wiley & Sons.

Svensson, L.; Heinegård, D, and Oldberg, Å. (1995) Decorin-binding sites for collagen type I are mainly located in leucine rich repeats 4-5. J. *Biol. Chem* 270, 20712-20716

Swatland, H.J., E. Gullet, T. Hore and S. Buttenham (1995). U.V. fibre-optic probe measurements in beef correlated with taste panel scores for chewiness. *Food Res. International*, Oxford 28: 23.

Uldbjerg, N., Ekman., G., Malmstrøm, A., Olsson, K. and Ulmsten (1983) Ripening om the human uterine cervix related to changes in collagen, glycosaminoglycans, and collagenolytic activity. *Am. J. Obstet. Gynecol*. 147, 216-219

Tornberg, E. (1996) Biophysical aspect of meat tenderness. *Meat Sci*. 43,175-191.

Van der Rest, M., and Garrone, R., (1991). Collagen family of proteins. *FASEB J*. 5:2814-2823.

Youling L. Xiong, Structure-Function relationships of Muscle Proteins.I: S.Damodaran and A.Paraf (eds), Food proteins and their application. University of Kentucky, Lexington, Kentucky.

Weber, I.T., Harrison, R.W. and Iozzo, R.V. (1996). Model structure of decorin and implications for collagen fibrillogenesis. *J. Biol. Chem*. 271: 31767-34770

Weston, A.R.; Rogers R. W.; PAS, and Althen, T.G.(2002)The role of collagen in meat tenderness. *The professional animal scientist*, 18 :107-111

Williams, D and Fleming, I. (2008) Spectroscopic methods in organic chemistry, 6th edition. UK: McGraw-Hill Higher Education,.